



Cite this: DOI: 10.1039/c4dt03021d

An expedient approach to synthesize fluorescent 3-substituted 4*H*-quinolizin-4-ones via (η^4 -vinylketene)-Fe(CO)₃ complexes†

Alfredo Rosas-Sánchez,^a Rubén A. Toscano,^b José G. López-Cortés^b and M. Carmen Ortega-Alfaro^{*a}

Received 1st October 2014,
Accepted 22nd October 2014

DOI: 10.1039/c4dt03021d
www.rsc.org/dalton

An efficient and practical methodology for the synthesis of 3-substituted 4*H*-quinolizin-4-ones using (η^4 -vinylketene)-Fe(CO)₃ complexes as key intermediates has been developed. The advantage of this transformation lies in the use of simple and readily available starting materials and mild carbonylation conditions. The fluorescent properties of these compounds were determined and the quantum yield was obtained, ranging from 0.04 to 0.36 depending on the substituent.

Introduction

Heterocyclic systems with a ring-junction nitrogen atom are of great interest due to the broad range of important biological and pharmaceutical applications that many of these derivatives exhibit.¹ Within this huge family of compounds, bicyclic systems such as 4*H*-quinolizin-4-one have shown antimicrobial,² antibacterial,³ antiallergic⁴ and HIV-integrase inhibitory⁵ activities, and other compounds exhibit interesting applications such as Mg²⁺-selective fluorescent indicators for intracellular 3D imaging.⁶ However, despite the potential applications of 4*H*-quinolizin-4-one derivatives, according to the literature only limited and non-general synthetic routes are known, and in some cases these require the use of drastic reaction conditions, multistep synthesis for obtaining appropriate starting materials or the use of highly expensive metals (*i.e.*, Pd or Rh), and include the disadvantage of poor global yields. Reported methods (Scheme 1) involve: (method A)⁷ intramolecular cyclization by thermolysis of α -substituted pyridine-*N*-oxides; (method B)⁸ acid-catalyzed annulation of quinoline-1-oxide with suitable substituted ylidemalonodinitriles; (method C)⁹ thermal ring closure of the α -substituted picones/ β , β -dichloroacrolein condensation product; (method D)¹⁰ nucleophilic addition of active methine compounds to cyclic

alkynylpyridine; (method E)¹¹ a multicomponent reaction/N-allylation/intramolecular Heck reaction sequence; (method F)¹² a Rh(III)-catalyzed double C–H activation and an oxidative coupling between primary benzamides and two alkyne units; and (method G)¹³ thermal rearrangement of 4-(2-pyridyl)-2-cyclobutenones.

Remarkably, transformations in methods A and G are thought to occur *via* intramolecular cyclization of the transient vinylketenes generated during the process; however spectroscopic evidence could not be obtained.

Since vinylketenes are usually unstable and highly reactive, the use of transition metals constitutes a powerful technique to stabilize this kind of intermediate, allowing to perform a large number of interesting transformations.¹⁴ In this context, isolable η^4 -vinylketene iron complexes can be obtained from vinylketone iron(0) complexes and used as precursors in different synthetic applications.¹⁵

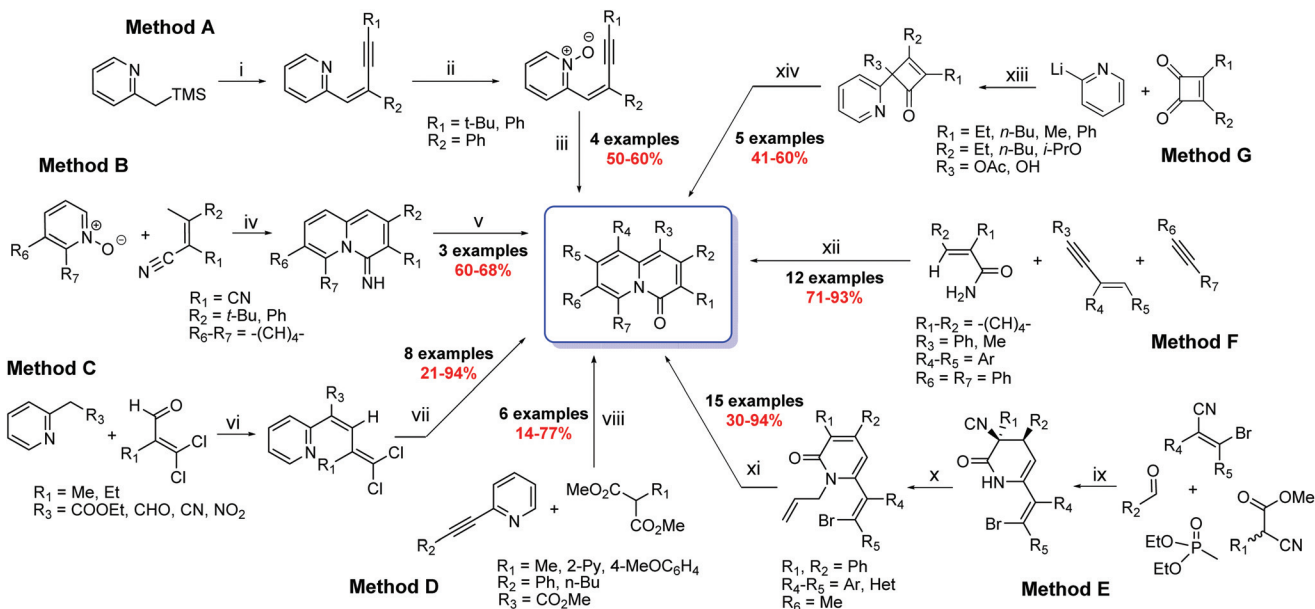
Recently, we reported the synthesis of an elusive ferrocenyl-vinylketene as a stable Fe(0) complex by means of the reaction of an [η^2 -(1-ferrocenyl-3-(2-pyridyl)-2E-propen-1-one)]-Fe(CO)₄ complex with MeLi under mild carbonylation conditions. The reactivity of this (η^4 -ferrocenylvinylketene)-Fe(CO)₃ complex, under thermal conditions, led to the formation of a 3-ferrocenyl-4*H*-quinolizin-4-one and the mechanism of this transformation was studied computationally within the DFT framework.¹⁶ As a logical extension of that work, we decided to replace the ferrocenyl fragment by different substituents including aryl and heterocyclic groups. Thereby, in this paper we report an efficient and concise alternative route to obtain 3-substituted 4*H*-quinolizin-4-ones from simple and readily available starting materials, using isolable and stable η^4 -(vinylketene)iron(0) complexes as key intermediates (Fig. 1). Interestingly, these new compounds **4** exhibit fluorescent

^aInstituto de Ciencias Nucleares, UNAM, Circuito Exterior, Ciudad Universitaria, Coyoacán, C.P. 04510, México D.F., México.

E-mail: carmen.ortega@nucleares.unam.mx

^bInstituto de Química, UNAM, Circuito Exterior, Ciudad Universitaria, Coyoacán, C.P. 04510, México D.F., México

† Electronic supplementary information (ESI) available. CCDC 1026201–1026206. For ESI and crystallographic data in CIF or other electronic format see DOI: 10.1039/c4dt03021d



Scheme 1 R_n in the quinolizinone system is H if it is not specified in the method. Yields shown in the scheme correspond to the last step. Reagents and conditions. **Method A:** (i) $R_1-C\equiv C-CO-R_2$, LDA, THF; (ii) MCPBA, $CHCl_3$; (iii) $380\text{ }^\circ C$. **Method B:** (iv) Ac_2O , Et_3N , 3 h; (v) H_3O^+ reflux, 2 h. **Method C:** (vi) 1. CH_3COOH , 0 $^\circ C$; 2. H_2O , 25 $^\circ C$, 16 h; (vii) dioxane: H_2O (1:1) reflux, 6 h. **Method D:** (viii) NaH , Diglyme, 150 $^\circ C$, 8–22 h. **Method E:** (ix) $nBuLi$, THF , –78 $^\circ C$ to rt; (x) NaH , allyl bromide, THF , 50 $^\circ C$; (xi) $Pd(OAc)_2$ 5%, Et_3N , DMF, 120 $^\circ C$, 16 h. **Method F:** (xii) $[Cp^*RhCl_2]_2$ 4%, Ag_2CO_3 , CH_3CN , 115 $^\circ C$, 12 h. **Method G:** (xiii) 1. THF , –78 $^\circ C$, 2. Ac_2O , 1.5 h, 3. $NaHCO_3$ (ac.); (xiv) 85 $^\circ C$ –100 $^\circ C$.

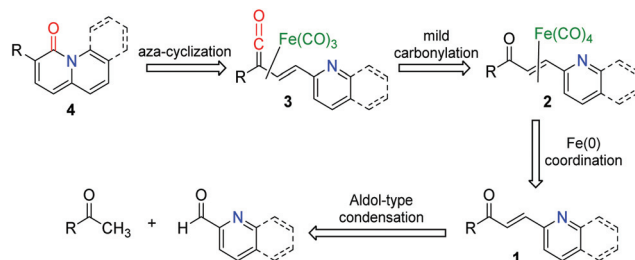


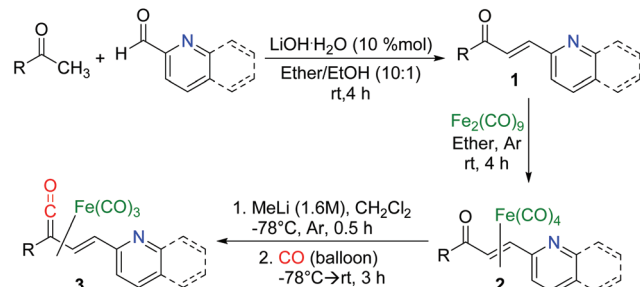
Fig. 1 Retrosynthetic strategy to 3-substituted 4*H*-quinolizin-4-ones.

properties, making them potential precursors for optical applications.

Results and discussion

Synthesis of (η^4 -vinylketene)- $Fe(CO)_3$ complexes 3

(η^4 -Vinylketene)- $Fe(CO)_3$ complexes 3 were obtained following the methodology described in Scheme 2. The starting materials 1-substituted 3-(2-pyridyl)-2*E*-propen-1-ones 1 were prepared through a base-catalyzed aldol-type condensation reaction between 2-pyridinecarbaldehyde and the corresponding ketone, in the presence of $LiOH \cdot H_2O$ under catalytic conditions.¹⁷ Satisfactory IR, NMR [1H , $^{13}C\{^1H\}$] and mass spectra were obtained for each synthesized compound. Subsequently, the α,β -unsaturated ketones 1a–l were coordinated to $Fe(0)$ in the presence of $Fe_2(CO)_9$,¹⁸ at room temperature, affording the corresponding (η^2 -PyCHCHCOR)- $Fe(CO)_4$ complexes 2. Additionally, in some cases it was possible to observe



Scheme 2 Synthesis of tricarbonyl(η^4 -vinylketene)iron(0) complexes 3.

the formation of (η^2 -PyCHCHCOR)- $Fe(CO)_3$ complexes as byproducts and the separation of both complexes could be achieved by flash column chromatography; however, this is unnecessary because the mixture of both complexes works well in the next transformation.

For the purpose of an unambiguous characterization, we undertook the isolation and purification of complexes 2, obtained as orange solids in moderate to good yields (Table 1), with the exception of 2k which readily decoordinates during the workup of the reaction. The formation of (η^2 -PyCHCHCOR)- $Fe(CO)_4$ complexes 2a–l was corroborated by 1H -NMR, where the chemical shifts of the coordinated olefinic protons attached to C_α and C_β are shifted upfield as two doublet signals at around 5.5 ppm and 5.0 ppm ($J \approx 10.2$ Hz) compared with the chemical shift of the same protons in the free ligands. In $^{13}C\{^1H\}$ -NMR, the chemical shift of the ketone still occurs around 190 ppm, while in IR spectroscopy it is possible to observe the $\nu(C=O)$ band around 1680 cm^{-1} , thus indicating

Table 1 Synthesis of complexes **2^a** and complexes **3^b**

Entry	1	R	Yield ^c (%)	
			2	3
1	1a	Ph	79 (2a) ^d	82 (3a)
2	1b	4-MeC ₆ H ₄	89 (2b)	76 (3b)
3	1c	4-BrC ₆ H ₄	87 (2c)	78 (3c)
4	1d	4-IC ₆ H ₄	83 (2d)	90 (3d)
5	1e	4-CF ₃ C ₆ H ₄	94 (2e)	47 (3e)
6	1f	4-MeOC ₆ H ₄	85 (2f)	80 (3f)
7	1g	4-PhC ₆ H ₄	82 (2g) ^d	77 (3g)
8	1h	2-Naphthyl	86 (2h)	83 (3h)
9	1i	2-(N-methylpyrrolyl)	85 (2i)	78 (3i)
10	1j	2-Furyl	86 (2j)	n.d. (3j) ^e
11	1k	2-Thienyl	n.d. (2k) ^e	n.d. (3k) ^e
12 ^f	1l	Ph	87 (2l)	73 (3l)

^a Conditions: **1** (1.0 mmol), Fe₂(CO)₉ (1.5 mmol). ^b Conditions: **2** (0.5 mmol), MeLi (1.1 equiv.), DCM (20 mL). ^c Isolated yields of complexes after purification. ^d Combined yield of η² and η⁴ complexes (η^2/η^4 ratio ~2:1 determined by ¹H-NMR). ^e Not determined (the complex decomposes readily so it was used in the next step without further purification). ^f 2-Quinolinicarboxaldehyde was used instead of 2-pyridinecarboxaldehyde.

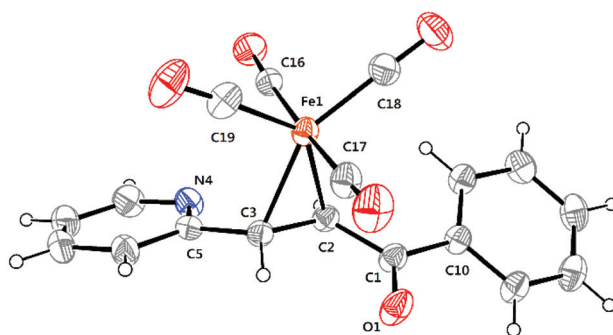


Fig. 2 ORTEP view of **2a** with thermal ellipsoids at 30% probability level. Selected bond lengths (Å) and angles (°): Fe(1)–C(18) 1.804(2); Fe(1)–C(19) 1.807(2); Fe(1)–C(16) 1.825(2); Fe(1)–C(17) 1.829(2); Fe(1)–C(2) 2.110(2); Fe(1)–C(3) 2.124(2); O(1)–C(1) 1.220(2); C(2)–C(3) 1.412(2); C(18)–Fe(1)–C(19) 116.34(10); C(18)–Fe(1)–C(16) 87.77(8); C(19)–Fe(1)–C(16) 90.18(9); C(18)–Fe(1)–C(17) 89.79(9); C(19)–Fe(1)–C(17) 89.15(9); C(16)–Fe(1)–C(17) 176.87(8); C(18)–Fe(1)–C(2) 108.18(8); C(19)–Fe(1)–C(2) 135.36(9); C(16)–Fe(1)–C(2) 88.37(7); C(17)–Fe(1)–C(2) 94.26(8); C(18)–Fe(1)–C(3) 146.79(9); C(19)–Fe(1)–C(3) 96.81(9); C(16)–Fe(1)–C(3) 94.37(7); C(17)–Fe(1)–C(3) 88.75(8); C(2)–Fe(1)–C(3) 38.97(6); C(3)–C(2)–Fe(1) 71.04(10); C(2)–C(3)–Fe(1) 69.99(10).

that the C=O bond in the ligand is not coordinated to the metallic fragment. The structures of **2a** (Fig. 2) and **2h** (see ESI†) were confirmed by X-ray single crystal diffraction. As noticed in ¹H and ¹³C{¹H}-NMR, the molecular structures reveal the coordination of the metal fragment only to the carbon–carbon double bond, with a slightly-distorted trigonal bipyramidal geometry around the iron atom and the C=C occupying an equatorial position, which is consistent with the results observed in other η²-(α,β-unsaturated ketones)-Fe(CO)₄ complexes.¹⁹

With complexes **2** in hand, we next undertook the synthesis of (η⁴-vinylketene)-Fe(CO)₃ complexes **3** under mild carbonylation

conditions.¹⁶ Complexes **3** were obtained as air and moisture stable compounds in moderate to good yields (Table 1). It is noteworthy that, in the case of [η²-(α,β-unsaturated ketones)]-Fe(CO)₄ complexes containing bromine and iodine as substituents, the possible halogen exchange promoted by MeLi was not observed. On the other hand, for ketenes containing heterocyclic substituents **3j–k** (Table 1, entries 10 and 11), the corresponding complexes were not isolated due to the degradation of the product during the workup of the reaction and the mixture was used in the next transformation without purification.

As expected, the IR spectra of (η⁴-vinylketene)-Fe(CO)₃ complexes show a middle-intensity absorption band around 1740 cm⁻¹ assigned to the vibrational frequency of the ketene group, while in ¹³C{¹H}-NMR spectroscopy, the chemical shift for the carbonyl carbon of the ketene (C=C=O) occurs down-field, at around 230 ppm. In ¹H-NMR, two doublet signals at around 7.40 ppm and 3.20 ppm as a coupled system with *J* ≈ 8.4 Hz are assigned to the hydrogens attached to *C*_α and *C*_β, respectively.

Additionally, the structure of **3g** was also confirmed by single crystal X-ray diffraction (Fig. 3).

The crystal structure of **3g** shows a distorted trigonal bipyramidal geometry around the iron atom due to the coordination to three CO ligands and a η⁴-coordination to the vinylketene through the four carbon atoms in the system. According to the gathered data, no significant differences in the geometry and bond distances around the ketene moiety can be seen with regard to other (η⁴-vinylketene)-Fe(CO)₃ complexes containing different substituents.^{15c,16,20}

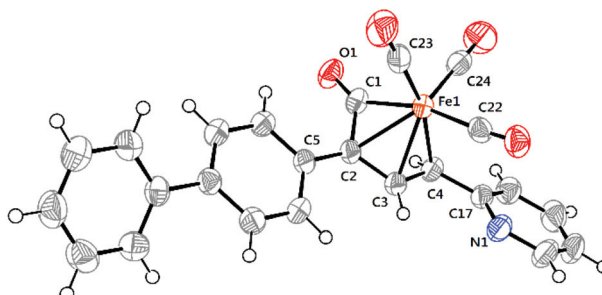


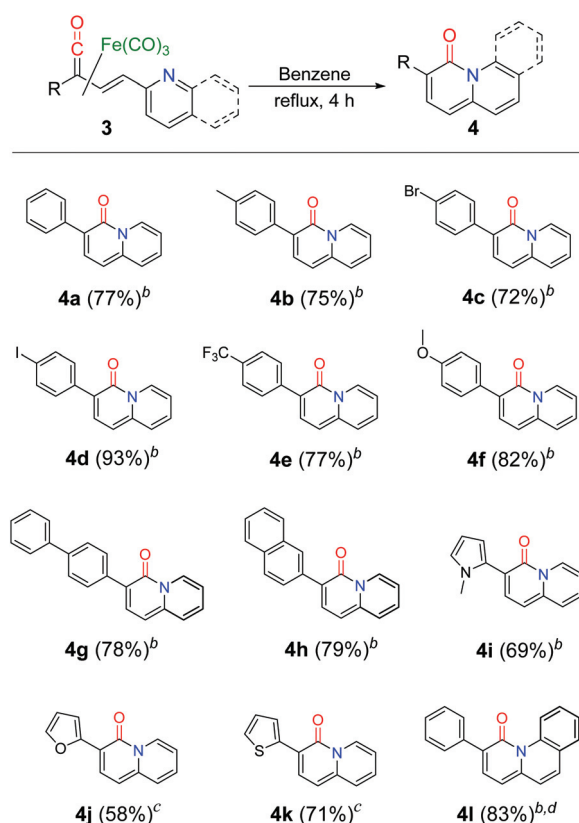
Fig. 3 ORTEP view of **3g** with thermal ellipsoids at 50% probability level. Selected bond lengths (Å) and angles (°): Fe(1)–C(24) 1.792(2); Fe(1)–C(23) 1.801(2); Fe(1)–C(22) 1.858(2); Fe(1)–C(1) 1.931(2); Fe(1)–C(2) 2.1522(18); Fe(1)–C(3) 2.1037(19); Fe(1)–C(4) 2.1612(19); C(1)–C(2) 1.474(3); C(2)–C(3) 1.412(2); C(3)–C(4) 1.415(3); C(2)–C(5) 1.481(3); C(4)–C(17) 1.481(3); C(24)–Fe(1)–C(23) 100.30(10); C(22)–Fe(1)–C(3) 93.83(8); C(23)–Fe(1)–C(4) 166.10(8); C(24)–Fe(1)–C(22) 98.51(9); C(1)–Fe(1)–C(3) 72.15(8); C(22)–Fe(1)–C(4) 93.82(8); C(23)–Fe(1)–C(22) 92.28(9); C(24)–Fe(1)–C(2) 134.92(9); C(1)–Fe(1)–C(4) 80.45(8); C(24)–Fe(1)–C(1) 96.80(9); C(23)–Fe(1)–C(2) 97.44(8); C(3)–Fe(1)–C(4) 38.73(7); C(23)–Fe(1)–C(1) 90.30(9); C(22)–Fe(1)–C(2) 121.86(8); C(2)–Fe(1)–C(4) 68.76(7); C(22)–Fe(1)–C(1) 163.75(8); C(1)–Fe(1)–C(2) 41.89(8); C(24)–Fe(1)–C(3) 129.16(9); C(23)–Fe(1)–C(3) 128.36(8); C(2)–C(1)–Fe(1) 77.10(11); C(3)–C(2)–Fe(1) 68.78(10); C(1)–C(2)–Fe(1) 61.01(10); C(3)–Fe(1)–C(2) 38.73(7); C(24)–Fe(1)–C(4) 91.14(9); C(2)–C(3)–Fe(1) 72.49(11); C(4)–C(3)–Fe(1) 72.83(11); C(3)–C(4)–Fe(1) 68.44(10).

Thermal cyclization of complexes 3

Finally, complexes 3 were refluxed in anhydrous benzene to promote intramolecular ring closure, affording the exclusive formation of 3-substituted 4*H*-quinolizin-4-ones 4 (Scheme 3). Good yields (72%–82%) were obtained for compounds **4a–h** bearing an electron-rich or an electron-deficient aryl group at the 3-position of the quinolizinone system, proving that no electronic effect disturbs this ring closure process. In the case of compounds with heterocyclic substituents, as mentioned above, decomposition of the corresponding (η^4 -vinylketene)- $\text{Fe}(\text{CO})_3$ complexes was observed during the workup of the reaction and the synthesis of quinolizinones **4j** and **4k** was performed without the purification of these intermediate complexes. Thus, the results obtained for **4j** and **4k** are described as global yield based on the corresponding α,β -unsaturated ketone.

The molecular structures of **4a**, **4d** (see ESI†) and **4e** (Fig. 4) were confirmed by X-ray diffraction analysis of suitable single crystals.

The crystal structures show a two-ring fused system with a bridge-head nitrogen atom essentially sp^2 hybridized, displaying a trigonal planar molecular geometry (sum of angles $\approx 360^\circ$); hence the lone pair in the pure *p* orbital on the nitrogen



Scheme 3 Scope of the 4*H*-quinolizin-4-one synthesis. Conditions: 3 (0.5 mmol), anhydrous benzene, reflux, 4 h. ^bIsolated yields. ^cGlobal yield from α,β -unsaturated ketone. ^dComplex 3l contains a 2-quinolyl group as a substituent instead of a 2-pyridyl group.

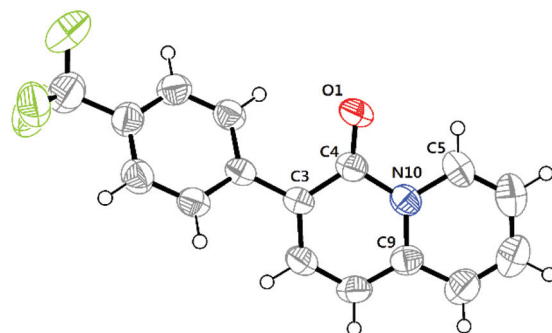


Fig. 4 ORTEP view of **4e** with thermal ellipsoids at 50% probability level. Selected bond lengths (Å) and angles (°): O(1)–C(4) 1.229(2); C(3)–C(4) 1.424(3); C(4)–N(10) 1.436(3); C(5)–N(10) 1.388(3); C(9)–N(10) 1.389(3); O(1)–C(4)–C(3) 127.2(2); O(1)–C(4)–N(10) 117.34(19); C(3)–C(4)–N(10) 115.48(18); C(5)–N(10)–C(9) 119.80(19); C(5)–N(10)–C(4) 116.76(18); C(9)–N(10)–C(4) 123.42(18).

is delocalized to contribute to the aromaticity in the molecule.²¹

As we have previously established by DFT calculations and experimental data,¹⁶ the [Fe(CO)₃] moiety not only stabilizes the vinylketene, but also helps in the *E/Z* isomerization of the vinyl fragment and serves as a coordination template, which explains the regiochemistry of this cyclic reaction.

Optical properties of 4*H*-quinolizin-4-ones 4

Although 4*H*-quinolizin-4-ones are of medical and pharmaceutical importance, we were interested in exploring their optical properties. Compounds **4** are yellow coloured and display bright yellow/green fluorescence in solution.

We acquired the absorption and emission spectra for compounds **4** (Fig. 5) observing that all compounds displayed maximum absorption in the visible region at λ_{abs} from 406 nm to 428 nm, with reasonable extinction coefficients ($\epsilon \approx 2 \times 10^4 \text{ M}^{-1} \text{ cm}^{-1}$), and broad maximum emission bands in the range of 480–530 nm at an excitation wavelength of 365 nm.

As can be seen from the Hammett plot²² in Fig. 6, there is a linear fit with a negative slope between the Hammett parameter for the *para*-substituent on the phenyl ring (σ_p^+)²³ and the Stokes shift observed in compounds **4a–g**. Substituents with net electron-withdrawing properties on the phenyl ring result in a shorter Stokes shift whereas net electron donating substituents result in larger values. On the other hand, compounds **4k**, **4i** and **4h** show Stokes shifts of 3284 cm⁻¹, 3721 cm⁻¹ and 4029 cm⁻¹ respectively, while compound **4l**, which has an additional ring fused to the quinolizinone system, exhibits the largest Stokes shift of 4876 cm⁻¹ (Table 2, entries 8–11). Regarding the emission intensity of 4*H*-quinolizin-4-ones, there is also a notable effect caused by the substitution patterns in the molecule. Compounds **4e** and **4g** containing –CF₃ and –Ph show the highest photoluminescence with quantum yields $\Phi = 0.36$ and 0.32, respectively (Table 2, entries 5 and 7). In contrast, compound **4l** shows the lowest emission intensity ($\Phi = 0.04$) in comparison with the analogous compound **4a** ($\Phi = 0.25$) (Table 2, entries 1 and 11).

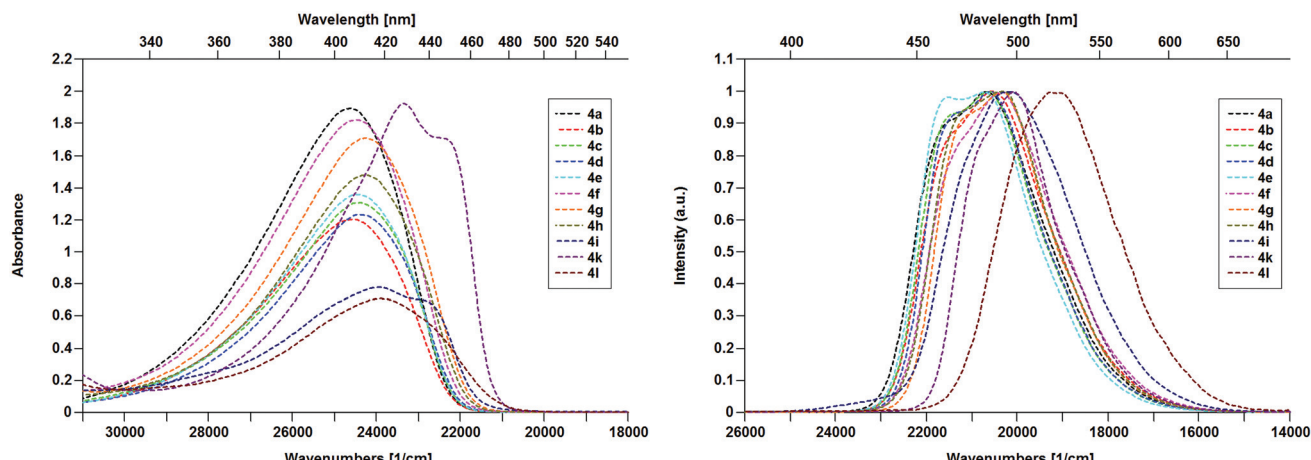


Fig. 5 UV–Vis absorption (left) and normalized emission (right) spectra of 4*H*-quinolizin-4-ones **4** in CHCl_3 . Absorbance at $c = 7 \times 10^{-4}$ M; emission at $c = 1 \times 10^{-4}$ M ($\lambda_{\text{ex}} = 365$ nm).

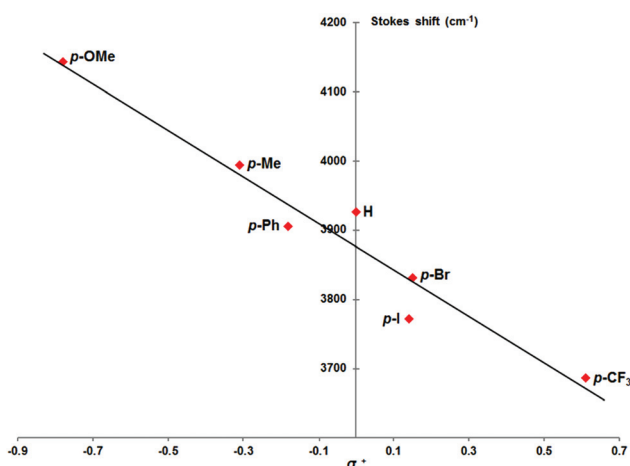


Fig. 6 Plot of the Hammett parameter vs. Stokes shift for compounds **4a–g**. (σ_p^+ for H = 0.0; Me = −0.31; Br = 0.15; I = 0.14; CF_3 = 0.61; OMe = −0.78; Ph = −0.18.)²³ Stokes shift = $-336.33\sigma_p^+ + 3876.3$, $R^2 = 0.9461$.

Table 2 Electronic absorption and photoluminescence of compounds **4**^a

Entry	4	λ_{abs}^b [nm]	$\epsilon^c \times 10^4$ [$\text{M}^{-1}\text{cm}^{-1}$]	λ_{em}^d [nm]	$\nu_{\text{abs}} - \nu_{\text{em}}^e$ [cm^{-1}]	ϕ^f
1	4a	406	2.72	483	3927	0.25
2	4b	407	1.66	486	3994	0.25
3	4c	409	1.92	485	3831	0.23
4	4d	410	1.68	485	3772	0.10
5	4e	410	1.79	483	3686	0.36
6	4f	408	2.52	491	4143	0.23
7	4g	412	2.41	491	3905	0.32
8	4h	412	2.05	494	4029	0.29
9	4i	418	1.06	495	3721	0.19
10	4k	428	2.67	498	3284	0.26
11	4l	418	0.99	525	4876	0.04

^a Compound **4j** decomposes in solution. ^b Absorption maxima in CHCl_3 at $c = 7 \times 10^{-4}$ M. ^c Molar extinction coefficient at absorption maxima. ^d Emission maxima in CHCl_3 at $c = 1 \times 10^{-4}$ M; $\lambda_{\text{ex}} = 365$ nm. ^e Stokes shift. ^f Quantum yields for emission in solution referred to quinine sulfate in 0.1 M H_2SO_4 ($\phi = 0.546$).

Further studies on the photophysics of these compounds are in progress and will be published in due course.

Conclusions

In summary, we have developed an efficient and practical methodology for the synthesis of 3-substituted 4*H*-quinolizin-4-ones in only four steps from simple and readily available starting materials. This methodology is based on a thermal intramolecular cyclization of (η^4 -vinylketene)- $\text{Fe}(\text{CO})_3$ complexes, where the $[\text{Fe}(\text{CO})_3]$ fragment plays an important role in stabilizing the highly reactive ketene group. Furthermore, this synthetic approach tolerates different kinds of aromatic rings, thus illustrating the scope of the reaction that, in principle, can be carried out with a vast number of α,β -unsaturated ketones containing a pyridine fragment. Moreover, this protocol has the additional advantage of requiring only mild reaction conditions, thus avoiding the use of cumbersome apparatus and highly expensive metal complexes.

Finally, this methodology provides a useful and alternative synthetic approach to interesting photoluminescent compounds that can be applied to a range of π -conjugated linear and cyclic structures and that could be used to design new assemblies of interest for organic light emitting diodes (OLEDs) and other electronic applications.

Experimental details

General considerations

All reagents and solvents were obtained from commercial suppliers and used without further purification. $\text{Fe}_2(\text{CO})_9$ was prepared using published methods.²⁴ Column chromatography was performed using 70–230 mesh silica gel. Yields are based on the pure products isolated. All the compounds were characterized by IR spectra recorded on a Perkin-Elmer Spectrum 100

FT-IR equipped with ATR accessory, and all data are expressed in wave numbers (cm^{-1}). Melting points were obtained on a Melt-Temp II apparatus and are uncorrected. NMR spectra were recorded with a Bruker Avance III, at 300 MHz using CDCl_3 as a solvent. Chemical shifts are in ppm (δ) relative to TMS. The following abbreviations are used: s = singlet, d = doublet, t = triplet, dd = double doublet, and m = multiplet. MS-EI spectra were obtained with a JEOL JMSAX505-HA using 70 eV as the ionization energy and, for MS-FAB, a JEOL JMS-SX102A using nitrobenzyl alcohol and ethylene glycol as a matrix.

Structure determination by X-ray crystallography

Suitable X-ray-quality crystals of **2a**, **2h**, **3g**, **4a**, **4d** and **4e** were grown by slow evaporation of a chloroform–benzene solvent mixture at -5°C . Single crystals of compounds **2a**, **2h**, **3g**, **4a**, **4d** and **4e** were mounted on a glass fiber at room temperature. The crystals were then placed on a Bruker SMART APEX CCD diffractometer equipped with Mo-K α radiation; decay was negligible in all cases. Details of the crystallographic data collected on compounds **2a**, **2h**, **3g**, **4a**, **4d** and **4e** are provided in Table 3. Systematic absences and intensity statistics were used in space group determinations. The structure was solved using direct methods.²⁵ Anisotropic structure refinements were achieved using full-matrix least-squares techniques on all non-hydrogen atoms. All hydrogen atoms were placed in idealized positions, on the basis of hybridization, with isotropic thermal parameters fixed at 1.2 times the value of the attached atom. Structure solutions and refinements were performed using SHELXTL v6.10.²⁶ Crystallographic data for **2a**, **2h**, **3g**, **4a**, **4d** and **4e** are available in CIF format in the ESI.†

UV-Vis absorption, photoluminescence (PL) spectroscopy and PL quantum yield (Φ) determination

CHCl_3 (spectrophotometric grade) was purchased from Sigma-Aldrich Co. and used without further purification. Absorption measurements were carried out at 298 K using a Varian Cary 100 UV-Vis spectrometer. Photoluminescence spectra were recorded at room temperature on a PerkinElmer LS-55 fluorescence spectrophotometer. The gradient method²⁷ was employed to estimate the photoluminescence quantum yield (Φ) of the samples using quinine sulfate in 0.1 M sulfuric acid at room-temperature as the reference fluorescent dye ($\Phi = 0.546$),²⁸ and by exciting all the samples at 365 nm, where the maximum intensity of emission was detected. Briefly, chloroform solutions at different concentrations of the samples were prepared, and their absorption and fluorescence spectra were recorded using a 10 mm optical path fluorescence cuvette. The concentration range of these solutions was such that their optical densities at the excitation wavelength (365 nm) were less than 0.1 to avoid self-absorption effects in the photoluminescence spectra.²⁹ The quantum yield for each sample was calculated using the following equation:

$$\Phi_X = \Phi_{\text{REF}} \left(\frac{m_X}{m_{\text{REF}}} \right) \left(\frac{n_X}{n_{\text{REF}}} \right)^2$$

where the subscripts X and REF denote the sample and the reference respectively, Φ is the photoluminescence quantum yield, n is the refractive index of the solvent, and m is the slope from the plot of integrated fluorescence intensity vs. absorbance.

Table 3 X-ray data collection and structure refinement details for compounds **2a**, **2h**, **3g**, **4a**, **4d** and **4e**

	2a	2h	3g	4a	4d	4e
Formula	$\text{C}_{18}\text{H}_{11}\text{FeNO}_5$	$\text{C}_{22}\text{H}_{13}\text{FeNO}_5$	$\text{C}_{24}\text{H}_{15}\text{FeNO}_4$	$\text{C}_{15}\text{H}_{11}\text{NO}$	$\text{C}_{16}\text{H}_{10}\text{INO}$	$\text{C}_{16}\text{H}_{10}\text{F}_3\text{NO}$
M_W (g^{-1} mol $^{-1}$)	377.13	427.18	437.22	221.25	347.14	289.25
Crystal size (mm 3)	$0.312 \times 0.296 \times 0.282$	$0.430 \times 0.326 \times 0.140$	$0.458 \times 0.292 \times 0.108$	$0.442 \times 0.403 \times 0.156$	$0.478 \times 0.232 \times 0.174$	$0.486 \times 0.264 \times 0.236$
Crystal system	Triclinic	Monoclinic	Triclinic	Orthorhombic	Monoclinic	Monoclinic
Space group	$P\bar{1}$	$P2_1/c$	$P\bar{1}$	$Pca2_1$	$P2_1/n$	$P2_1/c$
Cell parameters						
a (Å)	7.136(1)	10.5432(4)	9.1323(6)	15.2083(8)	6.492(4)	13.9430(15)
b (Å)	10.037(1)	15.2269(5)	10.4497(7)	6.5450(3)	21.091(13)	12.7966(14)
c (Å)	12.659(2)	12.0419(4)	11.6044(8)	21.7516(12)	9.629(6)	7.3613(8)
α (°)	92.570(2)	90	87.700(1)	90	90	90
β (°)	104.792(2)	91.721(1)	82.514(1)	90	102.311(10)	98.394(8)
γ (°)	105.483(2)	90	69.343(1)	90	90	90
V (Å 3)	838.51(18)	1932.34(12)	1027.36(12)	2165.12(19)	1288.1(14)	1299.4(4)
Z	2	4	2	8	4	4
d_c (Mg m $^{-3}$)	1.494	1.468	1.413	1.357	1.790	1.479
Reflections collected	9209	11 033	8848	13 809	10 484	10 269
Independent reflections, $R(\text{int})$	3065, 0.0206	35 440.0290	3736, 0.0436	4802, 0.0442	2368, 0.0629	2388, 0.0650
Data/parameters	3065/226	3544/262	3736/271	4802/307	2368/163	2388/247
Final R_1 , wR_2 [$I > 2\sigma(I)$]	0.0308, 0.0800	0.0349, 0.0868	0.0330, 0.0698	0.0563, 0.1249	0.0415, 0.0973	0.0534, 0.1072
R_1 , wR_2 (all data)	0.0332, 0.0818	0.0448, 0.0934	0.0414, 0.0737	0.0808, 0.1431	0.0548, 0.1033	0.0926, 0.1219
GoF on F^2	1.062	1.016	0.945	1.024	1.063	1.034
CCDC number	1026201	1026202	1026203	1026204	1026205	1026206

General procedure for the synthesis of α,β -unsaturated ketones 1a–l

The following procedure has been improved by modifying the methodology previously described in the literature:¹⁷ in a 50 mL round-bottomed flask, the corresponding methylketone (5.0 mmol) and 2-pyridinecarboxaldehyde (5.5 mmol) were dissolved in a solution of ethyl ether–EtOH (30 mL; ratio of ethyl ether–EtOH of 10 : 1, v/v) and treated with LiOH·H₂O (10% mol) under constant magnetic stirring at room temperature (~20–25 °C) until the starting material was consumed. In most cases, the reaction mixture turned yellow and the formation of a white precipitate was observed during reaction. After the completion of the reaction (3–4 h), the mixture was filtered through a neutral alumina/celite column (about 5 cm per phase) and the solvent was evaporated under reduced pressure using a rotary evaporator. The residue obtained was purified by column chromatography over silica gel using a hexane–ethyl acetate system (95 : 5, v/v) as an eluent to afford pure α,β -unsaturated ketones 1a–l.

(E)-1-Phenyl-3-(pyridin-2-yl)prop-2-en-1-one (1a). Light yellow solid (92%). m.p. 59–60 °C (Lit. 60–61 °C).³⁰ ATR-FTIR ν (cm^{−1}): 1663 (C=O), 1576 (C=C), 755, 688. ¹H-NMR (300 MHz, CDCl₃) δ (ppm): 8.64 (d, J = 4.7 Hz, 1H), 8.08 (d, J = 15.3 Hz, 1H), 8.05 (m, 2H), 7.73 (d, J = 15.3 Hz, 1H), 7.67 (m, 1H), 7.56–7.41 (m, 4H), 7.23 (m, 1H). ¹³C-NMR (75 MHz, CDCl₃) δ (ppm): 190.4, 153.2, 150.2, 142.8, 137.8, 136.9, 133.1, 128.8, 128.7, 125.5, 125.4, 124.5. MS (EI, 70 eV) m/z (%): 209 (64) [M]⁺, 180 (100) [M – HCO]⁺, 132 (41) [C₈H₆NO]⁺, 105 (22) [C₇H₅O]⁺, 104 (24) [C₇H₆N]⁺, 77 (30) [C₆H₅]⁺. HR-MS (FAB⁺) m/z for C₁₄H₁₂NO [M + H]⁺: calculated 210.0919, found 210.0924.

(E)-1-(4-Methylphenyl)-3-(pyridin-2-yl)prop-2-en-1-one (1b). Light yellow solid (85%). m.p. 61–62 °C (Lit. 67–68 °C).³¹ ATR-FTIR ν (cm^{−1}): 1658 (C=O), 1581 (C=C), 773. ¹H-NMR (300 MHz, CDCl₃) δ (ppm): 8.65 (d, J = 4.2 Hz, 1H), 8.09 (d, J = 15.3 Hz, 1H), 7.99 (d, J = 8.2 Hz, 2H), 7.74 (d, J = 15.2 Hz, 1H), 7.69 (m, 1H), 7.44 (d, J = 7.8 Hz, 1H), 7.30–7.20 (m, 3H), 2.39 (s, 3H). ¹³C-NMR (75 MHz, CDCl₃) δ (ppm): 189.9, 153.4, 150.2, 144.0, 142.4, 136.9, 135.4, 129.4, 129.0, 125.6, 125.4, 124.4, 21.8. MS (EI, 70 eV) m/z (%): 223 (78) [M]⁺, 194 (100) [M – HCO]⁺, 132 (23) [C₈H₆NO]⁺, 119 (28) [C₈H₇O]⁺, 104 (17) [C₇H₆N]⁺, 91 (21) [C₇H₇]⁺, 78 (9) [C₅H₄N]⁺. HR-MS (FAB⁺) m/z for C₁₅H₁₄NO [M + H]⁺: calculated 224.1075, found 224.1068.

(E)-1-(4-Bromophenyl)-3-(pyridin-2-yl)prop-2-en-1-one (1c). Light yellow solid (95%). m.p. 82–83 °C. ATR-FTIR ν (cm^{−1}): 1660 (C=O), 1581 (C=C), 766, 738. ¹H-NMR (300 MHz, CDCl₃) δ (ppm): 8.64 (d, 1H), 8.08 (d, J = 15.3 Hz, 1H), 8.06 (m, 2H), 7.74 (d, J = 15.3 Hz, 1H), 7.69 (m, 1H), 7.55–7.42 (m, 3H), 7.24 (m, 1H). ¹³C-NMR (75 MHz, CDCl₃) δ (ppm): 190.5, 153.2, 150.2, 142.9, 137.9, 136.9, 133.1, 128.8, 128.7, 125.6, 125.4, 124.5. MS (EI, 70 eV) m/z (%): 289, 287 (65) [M]⁺, 260, 258 (100) [M – HCO]⁺, 132(53) [C₈H₆NO]⁺, 185, 183 (20) [C₇H₄OBr]⁺, 104 (41) [C₇H₆N]⁺, 90 (18) [C₇H₇]⁺, 78 (21) [C₅H₄N]⁺. HR-MS (FAB⁺) m/z for C₁₄H₁₁BrNO [M + H]⁺: calculated 288.0024, found 288.0017.

(E)-1-(4-Iodophenyl)-3-(pyridin-2-yl)prop-2-en-1-one (1d). Light yellow solid (88%). m.p. 101–102 °C. ATR-FTIR ν (cm^{−1}): 1661 (C=O), 1578 (C=C), 775, 740. ¹H-NMR (300 MHz, CDCl₃) δ (ppm): 8.70 (d, J = 4.5 Hz, 1H), 8.08 (d, J = 15.3 Hz, 1H), 7.93–7.72 (m, 6H), 7.48 (d, J = 7.8 Hz, 1H), 7.38–7.29 (m, 1H). ¹³C-NMR (75 MHz, CDCl₃) δ (ppm): 189.5, 153.0, 150.2, 143.3, 138.0, 137.1, 137.0, 130.1, 125.7, 124.8, 124.6, 101.2. MS (EI, 70 eV) m/z (%): 335 (77) [M]⁺, 306 (100) [M – HCO]⁺, 231 (24) [C₇H₄IO]⁺, 203 (18) [C₆H₄I]⁺, 132 (33) [C₈H₆NO]⁺, 104 (28) [C₇H₆N]⁺, 76 (23) [C₆H₄]⁺. HR-MS (FAB⁺) m/z for C₁₄H₁₁INO [M + H]⁺: calculated 335.9885, found 335.9881.

(E)-3-(Pyridin-2-yl)-1-(4-(trifluoromethyl)phenyl)prop-2-en-1-one (1e). Light yellow solid (88%). m.p. 93–94 °C. IR (KBr) ν (cm^{−1}): 1662 (C=O), 1603 (C=C), 1111, 1062, 779. ¹H-NMR (300 MHz, CDCl₃) δ (ppm): 8.70 (d, J = 4.2 Hz, 1H), 8.19 (d, J = 8.1 Hz, 2H), 8.10 (d, J = 15.3 Hz, 1H), 7.83–7.74 (m, 4H), 7.49 (d, J = 7.8 Hz, 1H), 7.35–7.30 (m, 1H). ¹³C-NMR (75 MHz, CDCl₃) δ (ppm): 190.6, 152.9, 150.4, 144.0, 141.7, 137.1, 134.3 (q, J = 32.25 Hz, CCF₃), 129.1, 125.8, 125.7 (q, J = 3.75 Hz, CHCCF₃), 125.0, 124.9, 123.8 (q, J = 270.69, CF₃). MS (EI, 70 eV) m/z (%): 277 (34) [M]⁺, 248 (100) [M – HCO]⁺, 173 (12) [C₈H₄F₃O]⁺, 145 (27) [C₇H₄F₃]⁺, 132 (34) [C₈H₆NO]⁺, 104 (23) [C₇H₆N]⁺, 78 (13) [C₅H₄N]⁺. HR-MS (FAB⁺) m/z for C₁₅H₁₁F₃NO [M + H]⁺: calculated 278.0793, found 278.0795.

(E)-1-(4-Methoxyphenyl)-3-(pyridin-2-yl)prop-2-en-1-one (1f). Light yellow solid (82%). m.p. 67–68 °C (Lit. 71–72 °C).³¹ ATR-FTIR ν (cm^{−1}): 1659 (C=O), 1584 (C=C), 774, 742. ¹H-NMR (300 MHz, CDCl₃) δ (ppm): 8.69 (d, J = 4.6 Hz, 1H), 8.16–8.10 (m, 3H), 7.77 (d, J = 15.7 Hz, 1H), 7.73 (t, J = 7.7 Hz, 1H), 7.47 (d, J = 7.8 Hz, 1H), 7.29 (t, J = 6.1 Hz, 1H), 6.98 (d, J = 8.6 Hz, 2H), 3.88 (s, 3H). ¹³C-NMR (75 MHz, CDCl₃) δ (ppm): 188.7, 163.7, 153.4, 150.2, 142.0, 137.0, 131.2, 130.9, 125.5, 125.5, 124.4, 113.9, 55.6. MS (EI, 70 eV) m/z (%): 239 (74) [M]⁺, 210 (100) [M – HCO]⁺, 135 (76) [C₉H₇O₂]⁺, 132 (13) [C₈H₆NO]⁺, 104 (18) [C₇H₆N]⁺, 77 (21) [C₆H₅]⁺. HR-MS (FAB⁺) m/z for C₁₅H₁₄NO₂ [M + H]⁺: calculated 240.1025, found 240.1026.

(E)-1-[(1',1'-Biphenyl)-4-yl]-3-(pyridin-2-yl)prop-2-en-1-one (1g). Light yellow solid (88%). m.p. 139–140 °C. ATR-FTIR ν (cm^{−1}): 1660 (C=O), 1577 (C=C), 761, 688. ¹H-NMR (300 MHz, CDCl₃) δ (ppm): 8.69 (d, 1H), 8.18 (d, 2H), 8.17 (d, J = 15.3 Hz, 1H), 7.81 (d, J = 15.3 Hz, 1H), 7.75–7.62 (m, 5H), 7.46–7.38 (m, 4H), 7.28 (m, 1H). ¹³C-NMR (75 MHz, CDCl₃) δ (ppm): 190.0, 153.3, 150.3, 145.9, 142.8, 140.0, 137.0, 136.6, 129.5, 129.1, 128.4, 127.4, 125.6, 125.5, 124.6. MS (EI, 70 eV) m/z (%): 285 (60) [M]⁺, 256 (100) [M – HCO]⁺, 181 (18) [C₁₃H₉O]⁺, 152 (24) [C₁₂H₈]⁺, 132 (14) [C₈H₆NO]⁺, 104 (13) [C₇H₆N]⁺, 78 (8) [C₅H₄N]⁺. HR-MS (FAB⁺) m/z for C₂₀H₁₆NO [M + H]⁺: calculated 286.1232, found 286.1232.

(E)-1-(Naphthalen-2-yl)-3-(pyridin-2-yl)prop-2-en-1-one (1h). Light yellow solid (90%). m.p. 96–97 °C. IR (KBr) ν (cm^{−1}): 1658 (C=O), 1603 (C=C), 1322, 993, 782. ¹H-NMR (300 MHz, CDCl₃) δ (ppm): 8.70 (d, J = 4.2 Hz, 1H), 8.63 (s, 1H), 8.28 (d, J = 15.2 Hz, 1H), 8.15 (dd, J = 8.6, 1.5 Hz, 1H), 7.97 (d, J = 7.7 Hz, 1H), 7.91 (d, J = 8.6 Hz, 1H), 7.86 (d, J = 7.5 Hz, 2H), 7.83 (d, J = 15.2 Hz, 2H), 7.71 (td, J = 7.7, 1.6 Hz, 1H), 7.63–7.49 (m, 2H), 7.46 (d, J = 7.7 Hz, 1H), 7.27 (dd, J = 6.8, 5.5 Hz, 1H).

¹³C-NMR (75 MHz, CDCl₃) δ (ppm): 190.1, 153.2, 150.2, 142.6, 137.0, 135.7, 135.2, 132.6, 130.6, 129.7, 128.6, 128.6, 127.8, 126.8, 125.6, 125.4, 124.5, 124.5. MS (EI, 70 eV) m/z (%): 259 (43) [M]⁺, 230 (87) [M - HCO]⁺, 155 (45) [C₁₁H₇O]⁺, 132 (54) [C₈H₆NO]⁺, 127 (100) [C₁₁H₇]⁺, 104 (41) [C₇H₆N]⁺, 78 (35) [C₅H₄N]⁺. HR-MS (FAB⁺) m/z for C₁₈H₁₄NO [M + H]⁺: calculated 260.1075, found 260.1069.

(E)-1-(1-Methyl-1H-pyrrol-2-yl)-3-(pyridin-2-yl)prop-2-en-1-one (1i). In a round-bottomed flask, 1.0335 g (25.84 mmol) of NaOH were dissolved in 25 mL of a mixture of EtOH-H₂O (1 : 1, v/v). Subsequently, a solution of 2-acetyl-1-methylpyrrole (0.5 mL, 4.31 mmol) and 2-pyridinecarboxaldehyde (0.6 mL, 6.28 mmol) in 5 mL of ethanol was added dropwise at 0 °C and the reaction mixture was stirred for 24 h at room temperature (~20–25 °C). Later on, the ethanol was evaporated under reduced pressure using a rotary evaporator and the crude of the reaction was extracted with 30 mL of CH₂Cl₂. The organic phase was washed with 250 mL of distilled water and dried with anhydrous Na₂SO₄. Finally, the solvent was evaporated under reduced pressure using a rotary evaporator. The product was purified by column chromatography over silica gel using a hexane-ethyl acetate system (95 : 5, v/v) as an eluent. **3i** was obtained as a light yellow solid in 89% yield. m.p. 92–93 °C. ATR-FTIR ν (cm⁻¹): 1645 (C=O), 1599, 1578, 1468, 1403, 970, 730. ¹H-NMR (300 MHz, CDCl₃) δ (ppm): 8.66 (d, J = 4.4 Hz, 1H), 7.95 (d, J = 15.2 Hz, 1H), 7.76–7.63 (m, 2H), 7.43 (d, J = 7.7 Hz, 1H), 7.24 (m, 2H), 6.88 (s, 1H), 6.19 (m, 1H), 4.03 (s, 3H). ¹³C-NMR (75 MHz, CDCl₃) δ (ppm): 179.5, 153.6, 150.1, 139.8, 136.8, 132.1, 132.0, 127.4, 125.0, 124.0, 120.3, 108.5, 37.8. MS (EI, 70 eV) m/z (%): 212 (65) [M]⁺, 183 (100) [M - HCO]⁺, 134 (45) [C₈H₈NO]⁺, 132 (13) [C₈H₆NO]⁺, 108 (28) [C₆H₆NO]⁺, 104 (23) [C₇H₆N]⁺. HR-MS (FAB⁺) m/z for C₁₃H₁₃N₂O [M + H]⁺: calculated 213.1028, found 213.1029.

(E)-1-(Furan-2-yl)-3-(pyridin-2-yl)prop-2-en-1-one (1j).³² Light yellow solid (79%). m.p. 70–72 °C. ATR-FTIR ν (cm⁻¹): 1657 (C=O), 1611, 1577, 1464, 988, 766. ¹H-NMR (300 MHz, CDCl₃) δ (ppm): 8.69 (d, J = 4.5 Hz, 1H), 7.96 (d, J = 15.4 Hz, 1H), 7.83 (d, J = 15.4 Hz, 1H), 7.74 (td, J = 7.7, 1.8 Hz, 1H), 7.70–7.66 (m, 1H), 7.48 (d, J = 7.7 Hz, 1H), 7.42 (d, J = 3.6 Hz, 1H), 7.33–7.26 (m, 1H), 6.61 (dd, J = 3.6, 1.7 Hz, 1H). ¹³C-NMR (75 MHz, CDCl₃) δ (ppm): 177.9, 153.5, 152.9, 150.2, 147.1, 142.0, 136.9, 125.5, 124.9, 124.5, 118.4, 112.6. MS (EI, 70 eV) m/z (%): 200 (97) [M + 1]⁺, 170 (100) [M - H₂CO]⁺, 132 (31) [C₈H₆NO]⁺, 117 (86) [C₈H₇N]⁺, 104 (30) [C₇H₆N]⁺, 95 (22) [C₅H₃O₂]⁺, 78 (16) [C₅H₄N]⁺. HR-MS (FAB⁺) m/z for C₁₂H₁₀NO₂ [M + H]⁺: calculated 200.0712, found 200.0718.

(E)-3-(Pyridin-2-yl)-1-(thiophen-2-yl)prop-2-en-1-one (1k). Light yellow solid (83%). m.p. 78–79 °C. ATR-FTIR ν (cm⁻¹): 1646 (C=O), 1597, 1514, 1408, 1326, 978, 736. ¹H-NMR (300 MHz, CDCl₃) δ (ppm): 8.69 (d, J = 4.3 Hz, 1H), 8.00 (d, J = 15.4 Hz, 1H), 7.96 (d, J = 4.3 Hz, 1H), 7.80 (d, J = 15.3 Hz, 1H), 7.75–7.68 (m, 2H), 7.47 (d, J = 7.7 Hz, 1H), 7.30 (m, 1H), 7.18 (t, J = 4.3 Hz, 1H). ¹³C-NMR (75 MHz, CDCl₃) δ (ppm): 182.3, 153.0, 150.2, 145.6, 142.1, 137.0, 134.5, 132.6, 128.4, 125.7, 125.3, 124.6. MS (EI, 70 eV) m/z (%): 215 (28) [M]⁺, 186 (100) [M - HCO]⁺, 132 (13) [C₈H₆NO]⁺, 111 (50) [C₅H₃OS]⁺, 104 (28)

[C₇H₆N]⁺, 78 (13) [C₅H₄N]⁺. HR-MS (FAB⁺) m/z for C₁₂H₁₀NOS [M + H]⁺: calculated, 216.0483 found 216.0490.

(E)-1-Phenyl-3-(quinolin-2-yl)prop-2-en-1-one (1l). Light yellow solid (89%). m.p. 118–119 °C. IR (KBr) ν (cm⁻¹): 1658 (C=O), 1595 (C=C), 1250, 772, 696. ¹H-NMR (300 MHz, CDCl₃) δ (ppm): 8.26–8.07 (m, 5H), 7.95 (d, J = 15.6 Hz, 1H), 7.81 (d, J = 8.1 Hz, 1H), 7.74 (t, J = 7.9 Hz, 1H), 7.65 (d, J = 8.2 Hz, 1H), 7.62–7.48 (m, 4H). ¹³C-NMR (75 MHz, CDCl₃) δ (ppm): 190.7, 153.5, 148.4, 143.7, 137.9, 136.9, 133.2, 130.2, 129.9, 128.9, 128.7, 128.3, 127.7, 127.4, 127.1, 121.5. MS (EI, 70 eV) m/z (%): 259 (39) [M]⁺, 230 (100) [M - HCO]⁺, 182 (41) [C₁₂H₈O]⁺, 154 (21) [C₁₁H₈N]⁺, 105 (15) [C₇H₅O]⁺, 77 (18) [C₆H₅]⁺. HR-MS (FAB⁺) m/z for C₁₈H₁₄NO [M + H]⁺: calculated 260.1075, found 260.1084.

General procedure for the synthesis of [η^2 -(α,β -unsaturated ketones)]-Fe(CO)₄ complexes 2a–l

In a 50 mL dried round-bottomed flask, a solution of **1** (1 mmol) in anhydrous ethyl ether (20 mL per mmol) was treated with Fe₂(CO)₉ (1.5 mmol) under an inert atmosphere and magnetic stirring at room temperature (~20–25 °C). After 4 h, the reaction mixture was filtered through a neutral alumina/celite column (about 5 cm per phase) and the solvent was evaporated under reduced pressure using a rotary evaporator. The reaction mixture without purification was then used for the next transformation. However, with the purpose of an unambiguous identification, some of the η^2 -[Fe(CO)₄] complexes were purified by silica gel column chromatography (CC) using hexane-ethyl acetate (7 : 3, v/v) as an eluent.

η^2 -[(E)-1-Phenyl-3-(pyridin-2-yl)-2-propen-1-one] tetracarbonyliron(0) (2a). Orange-red solid (79%). m.p. (dec.) 75–80 °C. ATR-FTIR ν (cm⁻¹): 2090, 2067, 2009, 1976 (M-C≡O), 1684 (C=O). ¹H-NMR (300 MHz, CDCl₃) δ (ppm): 8.34 (s, 1H), 8.17 (s, 2H), 7.52 (s, 4H), 7.40 (s, 1H), 6.98 (s, 1H), 5.48 (s, 1H), 4.95 (s, 1H). ¹³C-NMR (75 MHz, CDCl₃) δ (ppm): 206.5, 196.4, 161.4, 149.1, 137.6, 136.7, 132.6, 128.6, 128.0, 123.3, 121.4, 57.1, 49.9. MS (FAB⁺) m/z (%): 378 (31) [M + 1]⁺, 349 (10) [M - CO]⁺, 321 (29) [M - 2CO]⁺, 393 (67) [M - 3CO]⁺, 265 (70) [M - 4CO]⁺, 210 (45) [M + 1-Fe(CO)₄]⁺, 180 (55) [M - H₂CO]⁺. HR-MS (FAB⁺) m/z for C₁₈H₁₂FeNO₅ [M + H]⁺: calculated 378.0065, found 378.0066.

η^2 -[(E)-1-(4-Methylphenyl)-3-(pyridin-2-yl)-2-propen-1-one]-tetracarbonyliron(0) (2b). Orange-red solid (89%). m.p. (dec.) 80–85 °C. ATR-FTIR ν (cm⁻¹): 2065, 2089, 2010, 1980 (M-C≡O), 1681 (C=O), 770, 738, 827. ¹H-NMR (300 MHz, CDCl₃) δ (ppm): 8.34 (s, 1H), 8.07 (s, 2H), 7.54 (s, 1H), 7.38 (s, 1H), 7.28 (s, 2H), 6.98 (s, 1H), 5.46 (s, 1H), 4.94 (s, 1H), 2.40 (s, 3H). ¹³C-NMR (75 MHz, CDCl₃) δ (ppm): 206.5, 195.9, 161.5, 149.0, 143.4, 136.6, 134.9, 129.3, 128.2, 123.2, 121.3, 57.1, 50.0, 21.7. MS (FAB⁺) m/z (%): 392 (53) [M + 1]⁺, 363 (14) [M - CO]⁺, 335 (32) [M - 2CO]⁺, 307 (96) [M - 3CO]⁺, 279 (86) [M - 4CO]⁺, 224 (57) [M + 1-Fe(CO)₄]⁺. HR-MS (FAB⁺) m/z for C₁₉H₁₄FeNO₅ [M + H]⁺: calculated 392.0221, found 392.0215.

η^2 -[(E)-1-(4-Bromophenyl)-3-(pyridin-2-yl)-2-propen-1-one]-tetracarbonyliron(0) (2c). Orange-red solid (87%). m.p. (dec.) 80–85 °C. ATR-FTIR ν (cm⁻¹): 2091, 2066, 2010, 1985 (M-C≡O),

1685 (C=O), 779, 741. $^1\text{H-NMR}$ (300 MHz, CDCl_3) δ (ppm): 8.37 (s, 1H), 8.06 (s, 2H), 7.61–7.67 (m, 3H), 7.44 (s, 1H), 7.04 (s, 1H), 5.42 (d, J = 10.2 Hz, 1H), 4.95 (d, J = 10.2 Hz, 1H). $^{13}\text{C-NMR}$ (75 MHz, CDCl_3) δ (ppm): 206.2, 195.2, 161.2, 149.1, 136.8, 136.2, 132.0, 129.6, 127.7, 123.3, 121.5, 56.9, 49.5. MS (FAB $^+$) m/z (%): 458, 456 (12) [M + 1] $^{+*}$, 373, 371 (43) [M – 3CO] $^+$, 345, 343 (60) [M – 4CO] $^+$, 290, 288 (325) [M + 1-Fe(CO) $_4$] $^+$. HR-MS (FAB $^+$) m/z for $\text{C}_{18}\text{H}_{11}\text{BrFeNO}_5$ [M + H] $^+$: calculated 455.9170, found 455.9174.

η^2 -[(E)-1-(4-Iodophenyl)-3-(pyridin-2-yl)-2-propen-1-one]tetracarbonyliron(0) (2d). Orange-red solid (83%). m.p. (dec.) 75–80 °C. ATR-FTIR ν (cm $^{-1}$): 2091, 2066, 2010, 1982 (M-C≡O), 1686 (C=O), 778, 738. $^1\text{H-NMR}$ (300 MHz, CDCl_3) δ (ppm): 8.37 (d, 1H), 7.89–7.80 (m, 4H), 7.60 (s, 1H), 7.43 (d, 1H), 7.03 (t, 1H), 5.41 (d, J = 10.2 Hz, 1H), 4.95 (d, J = 10.2 Hz, 1H). $^{13}\text{C-NMR}$ (75 MHz, CDCl_3) δ (ppm): 206.2, 195.5, 161.2, 149.1, 138.0, 136.8, 129.6, 123.4, 121.6, 100.5, 56.9, 49.5. MS (FAB $^+$) m/z (%): 504 (12) [M + 1] $^{+*}$, 475 (7) [M – CO] $^+$, 448 (17) [M + 1-2CO] $^+$, 419 (33) [M – 3CO] $^+$, 391 (57) [M – 4CO] $^+$, 336 (21) [M + 1-Fe(CO) $_4$] $^+$. HR-MS (FAB $^+$) m/z for $\text{C}_{18}\text{H}_{11}\text{IFeNO}_5$ [M + H] $^+$: calculated 503.9031, found 503.9031.

η^2 -[(E)-3-(Pyridin-2-yl)-1-(4-(trifluoromethyl)phenyl)prop-2-en-1-one]tetracarbonyliron(0) (2e). Orange-red solid (94%). m.p. (dec.) 90–95 °C. ATR-FTIR ν (cm $^{-1}$): 2095, 2072, 2016, 1987 (M-C≡O), 1664 (C=O), 1635, 1316, 1109, 1065, 780. $^1\text{H-NMR}$ (300 MHz, CDCl_3) δ (ppm): 8.38 (d, J = 4.2 Hz, 1H), 8.30 (d, J = 8.1 Hz, 2H), 7.79 (d, J = 8.2 Hz, 2H), 7.61 (td, J = 7.7, 1.7 Hz, 1H), 7.45 (d, J = 7.8 Hz, 1H), 7.10–6.98 (m, 1H), 5.46 (d, J = 10.4 Hz, 1H), 4.97 (d, J = 10.4 Hz, 1H). $^{13}\text{C-NMR}$ (75 MHz, CDCl_3) δ (ppm): 206.0, 195.2, 161.1, 149.1, 140.5, 136.8, 134.0 (q, J = 32.3 Hz, CF_3), 128.4, 125.8 (q, J = 3.7 Hz, CHCCF_3), 123.9 (q, J = 270.8 Hz, CF_3), 123.4, 121.6, 56.9, 49.7. MS (FAB $^+$) m/z (%): 446 (25) [M + 1] $^{+*}$, 418 (18) [M + 1-CO] $^+$, 390 (30) [M + 1-2CO] $^+$, 362 (55) [M + 1-3CO] $^+$, 333 (100) [M – 4CO] $^+$, 278 (55) [M + 1-Fe(CO) $_4$] $^+$. HR-MS (FAB $^+$) m/z for $\text{C}_{19}\text{H}_{11}\text{F}_3\text{FeNO}_5$ [M + H] $^+$: calculated 445.9939, found 445.9946.

η^2 -[(E)-1-(4-Methoxyphenyl)-3-(pyridin-2-yl)-2-propen-1-one]tetracarbonyliron(0) (2f). Orange-red solid (85%). m.p. (dec.) 85–90 °C. ATR-FTIR ν (cm $^{-1}$): 2091, 2064, 2012, 1980 (M-C≡O), 1661 (C=O), 843. $^1\text{H-NMR}$ (300 MHz, CDCl_3) δ (ppm): 8.37 (s, 1H), 8.20 (d, J = 8.2 Hz, 2H), 7.59 (m, 1H), 7.42 (d, J = 7.4 Hz, 1H), 7.00 (d, J = 7.7 Hz, 3H), 5.50 (d, J = 10.4 Hz, 1H), 4.97 (d, J = 10.4 Hz, 1H), 3.89 (s, 3H). $^{13}\text{C-NMR}$ (75 MHz, CDCl_3) δ (ppm): 206.7, 195.0, 163.3, 161.6, 149.0, 136.7, 130.4, 130.3, 123.3, 121.3, 113.9, 57.2, 55.6, 49.9. MS (FAB $^+$) m/z (%): 408 (29) [M + 1] $^{+*}$, 380 (8) [M – CO] $^+$, 352 (36) [M – 2CO] $^+$, 323 (100) [M – 3CO] $^+$, 295 (92) [M – 4CO] $^+$, 240 (44) [M + 1-Fe(CO) $_4$] $^+$. HR-MS (FAB $^+$) m/z for $\text{C}_{19}\text{H}_{14}\text{FeNO}_6$ [M + H] $^+$: calculated 408.0171, found 408.0171.

η^2 -[(E)-1-((1,1'-Biphenyl)-4-yl)-3-(pyridin-2-yl)-2-propen-1-one]tetracarbonyliron(0) (2g). Orange-red solid (82%). m.p. (dec.) 65–70 °C. ATR-FTIR ν (cm $^{-1}$): 2089, 2068, 2010, 1983 (M-C≡O), 1626 (C=O). $^1\text{H-NMR}$ (300 MHz, CDCl_3) δ (ppm): 8.38 (d, 1H), 8.28 (d, 2H), 7.77–7.64 (m, 5H), 7.48–7.43 (m, 4H), 7.03 (m, 1H), 5.55 (d, J = 10.5 Hz, 1H), 4.99 (d, J = 10.4 Hz, 1H). $^{13}\text{C-NMR}$ (75 MHz, CDCl_3) δ (ppm): 206.4, 195.8,

161.4, 149.0, 145.3, 140.1, 138.8, 136.2, 129.0, 128.6, 128.2, 127.3, 127.2, 123.2, 121.4, 57.0, 49.9. MS (FAB $^+$) m/z (%): 454 (10) [M + 1] $^{+*}$, 426 (4) [M – CO] $^+$, 398 (10) [M – 2CO] $^+$, 370 (28) [M – 3CO] $^+$, 342 (52) [M – 4CO] $^+$, 286 (34) [M + 1-Fe(CO) $_4$] $^+$. HR-MS for $\text{C}_{24}\text{H}_{16}\text{FeNO}_5$ [M + H] $^+$: calculated 454.0378, found 454.0371.

η^2 -[(E)-1-(Naphthalen-2-yl)-3-(pyridin-2-yl)-2-propen-1-one]tetracarbonyliron(0) (2h). Orange-red solid (86%). m.p. (dec.) 115–120 °C. IR (KBr) ν (cm $^{-1}$): 2094, 2064, 2037, 1983 (M-C≡O), 1631 (C=O), 1582, 1466, 750, 613. $^1\text{H-NMR}$ (300 MHz, CDCl_3) δ (ppm): 8.77 (s, 1H), 8.41 (s, 1H), 8.24 (s, 1H), 8.03–7.89 (m, 3H), 7.58–7.46 (m, 4H), 7.02 (s, 1H), 5.67 (d, J = 9.5 Hz, 1H), 5.05 (d, J = 9.5 Hz, 1H). $^{13}\text{C-NMR}$ (75 MHz, CDCl_3) δ (ppm): 206.5, 196.2, 161.5, 149.1, 136.8, 135.6, 134.8, 132.9, 129.7, 129.3, 128.5, 128.3, 127.9, 126.8, 124.4, 123.4, 121.5, 57.2, 50.2. MS (FAB $^+$) m/z (%): 428 (27) [M + 1] $^{+*}$, 372 (32) [M + 1-2CO] $^+$, 343 (47) [M – 3CO] $^+$, 316 (100) [M + 1-4CO] $^+$, 260 (33) [M + 1-Fe(CO) $_4$] $^+$. HR-MS (FAB $^+$) m/z for $\text{C}_{22}\text{H}_{14}\text{FeNO}_5$ [M + H] $^+$: calculated 428.0221, found 428.0216.

η^2 -[(E)-1-(1-Methyl-1H-pyrrrol-2-yl)-3-(pyridin-2-yl)-2-propen-1-one]tetracarbonyliron(0) (2i). Orange-red solid (85%). m.p. (dec.) 100–105 °C. ATR-FTIR ν (cm $^{-1}$): 2090, 2016, 1964 (M-C≡O), 1652 (C=O), 1616, 1585, 1470, 1403, 735. $^1\text{H-NMR}$ (300 MHz, CDCl_3) δ (ppm): 8.36 (s, 1H), 7.54 (d, J = 7.1 Hz, 1H), 7.38 (s, 2H), 6.98 (s, 1H), 6.82 (s, 1H), 6.21 (s, 1H), 5.46 (d, J = 10.5 Hz, 1H), 4.88 (d, J = 10.5 Hz, 1H), 3.95 (s, 3H). $^{13}\text{C-NMR}$ (75 MHz, CDCl_3) δ (ppm): 207.2, 187.6, 161.8, 149.0, 136.6, 130.8, 130.7, 123.0, 121.1, 118.2, 108.2, 57.0, 52.1, 37.8. MS (FAB $^+$) m/z (%): 381 (15) [M + 1] $^{+*}$, 352 (6) [M – CO] $^+$, 324 (15) [M – 2CO] $^+$, 296 (58) [M – 3CO] $^+$, 268 (39) [M – 4CO] $^+$, 213 (26) [M + 1-Fe(CO) $_4$] $^+$. HR-MS (FAB $^+$) m/z for $\text{C}_{17}\text{H}_{13}\text{FeN}_2\text{O}_5$ [M + H] $^+$: calculated 381.0174, found 381.0179.

η^2 -[(E)-1-(Furan-2-yl)-3-(pyridin-2-yl)-2-propen-1-one]tetracarbonyliron(0) (2j). Orange-red solid (86%). m.p. (dec.) 95–100 °C. ATR-FTIR ν (cm $^{-1}$): 2088, 2006, 1977, 1950 (M-C≡O), 1622 (C=O), 1566, 1465, 1319, 1012, 757. $^1\text{H-NMR}$ (300 MHz, CDCl_3) δ (ppm): 8.38 (s, 1H), 7.66 (s, 1H), 7.58 (s, 1H), 7.40 (d, J = 7.1 Hz, 1H), 7.35 (s, 1H), 7.02 (s, 1H), 6.59 (s, 1H), 5.46 (d, J = 10.4 Hz, 1H), 4.94 (d, J = 10.3 Hz, 1H). $^{13}\text{C-NMR}$ (75 MHz, CDCl_3) δ (ppm): 206.4, 185.4, 161.3, 152.95, 149.1, 145.9, 136.7, 123.1, 121.4, 116.2, 112.5, 56.1, 49.8. MS (FAB $^+$) m/z (%): 368 (45) [M + 1] $^{+*}$, 339 (18) [M – CO] $^+$, 311 (49) [M – 2CO] $^+$, 283 (85) [M – 3CO] $^+$, 255 (70) [M – 4CO] $^+$, 200 (53) [M + 1-Fe(CO) $_4$] $^+$. HR-MS (FAB $^+$) m/z for $\text{C}_{16}\text{H}_{10}\text{FeNO}_6$ [M + H] $^+$: calculated 367.9858, found 367.9858.

η^2 -[(E)-1-Phenyl-3-(quinolin-2-yl)-2-propen-1-one]tetracarbonyliron(0) (2l). Orange-red solid (87%). m.p. (dec.) 100–105 °C. IR (KBr) ν (cm $^{-1}$): 2094, 2067, 2017, 1984 (M-C≡O), 1632 (C=O), 1291, 591. $^1\text{H-NMR}$ (300 MHz, CDCl_3) δ (ppm): 8.27 (d, J = 7.1 Hz, 2H), 8.06 (d, J = 8.5 Hz, 1H), 7.86 (d, J = 8.4 Hz, 1H), 7.73 (d, J = 8.0 Hz, 1H), 7.68–7.48 (m, 5H), 7.47–7.35 (m, 1H), 5.78 (d, J = 10.4 Hz, 1H), 5.04 (d, J = 10.4 Hz, 1H). $^{13}\text{C-NMR}$ (75 MHz, CDCl_3) δ (ppm): 206.1, 196.5, 162.0, 147.7, 137.6, 136.6, 132.8, 129.8, 128.8, 128.4, 128.2, 127.8, 127.1, 125.9, 122.1, 56.9, 50.1. MS (FAB $^+$) m/z (%): 428 (23) [M + 1] $^{+*}$, 372 (30) [M + 1-2CO] $^+$, 344 (47) [M + 1-3CO] $^+$,

315 (100) $[M - 4CO]^+$, 260 (40) $[M + 1-Fe(CO)_4]^+$. HR-MS (FAB $^+$) m/z for $C_{22}H_{14}FeNO_5$ $[M + H]^+$: calculated 428.0221, found 428.0223.

General procedure for the synthesis of (η^4 -vinylketene)-Fe(CO)₃ complexes 3a–l

In a 50 mL dried round-bottomed flask, MeLi (1.1 equiv., 1.6 M) was added dropwise to a solution of 2 (0.5 mmol) in anhydrous dichloromethane (20 mL) at –78 °C under an inert atmosphere. The reaction mixture was stirred for 30 min before proceeding to exchange the inert atmosphere for CO at atmospheric pressure. The mixture was stirred for another 30 min at –78 °C and, after that, the temperature was allowed to rise slowly to room temperature until 4 h had elapsed. After the reaction was complete, the crude product was filtered through a celite column (5 cm), and the solvent was evaporated under reduced pressure using a rotary evaporator. The reaction mixture was chromatographed on a flash column over silica gel using hexane–dichloromethane (6 : 4, v/v) as an eluent.

η^4 -[(E)-2-Phenyl-4-(pyridin-2-yl)-1,3-butadien-1-one]tricarbonyliron(0) (3a). Orange solid (82%). m.p. (dec.) 116–117 °C. ATR-FTIR ν (cm $^{-1}$): 2058, 1991, 1961 (C=O)_{metallic}, 1730 (C=O)_{ketene}. 1 H-NMR (300 MHz, CDCl $_3$) δ (ppm): 8.62 (d, J = 3.9 Hz, 1H), 7.63 (dd, J = 18.4, 7.4 Hz, 3H), 7.50–7.29 (m, 4H), 7.24 (d, J = 8.4 Hz, 1H), 7.20–7.09 (m, 1H), 3.28 (d, J = 8.4 Hz, 1H). 13 C-NMR (75 MHz, CDCl $_3$) δ (ppm): 233.5, 157.4, 150.0, 136.9, 131.1, 129.4, 129.4, 127.6, 123.1, 122.0, 94.2, 57.9, 50.9. MS (FAB $^+$) m/z (%): 362 (5) $[M + 1]^+$, 334 (6) $[M + 1-CO]^+$, 306 (5) $[M + 1-2CO]^+$, 277 (45) $[M - 3CO]^+$, 249 (35) $[M - 4CO]^+$, 193 (100) $[M - Fe(CO)_4]^+$. HR-MS (FAB $^+$) m/z for $C_{15}H_{11}FeNO$ $[M - 3CO]^+$: calculated 277.0190, found 277.0194.

η^4 -[(E)-4-(Pyridin-2-yl)-2-(*p*-tolyl)-1,3-butadien-1-one]tricarbonyliron(0) (3b). Orange solid (76%). m.p. (dec.) 120–122 °C. ATR-FTIR ν (cm $^{-1}$): 2063, 2005, 1981 (C=O)_{metallic}, 1742 (C=O)_{ketene}. 1 H-NMR (300 MHz, CDCl $_3$) δ (ppm): 8.62 (d, J = 4.2 Hz, 1H), 7.65–7.56 (m, 2H), 7.55 (s, 1H), 7.42 (d, J = 8.4 Hz, 1H), 7.25 (d, J = 4.6 Hz, 1H), 7.21 (d, J = 7.8 Hz, 2H), 7.15 (m, 1H), 3.25 (d, J = 8.4 Hz, 1H), 2.36 (s, 3H). 13 C-NMR (75 MHz, CDCl $_3$) δ (ppm): 234.1, 157.6, 150.0, 139.3, 136.9, 130.1, 127.7, 127.5, 123.1, 121.9, 93.9, 57.6, 51.3, 21.5. MS (FAB $^+$) m/z (%): 376 (6) $[M + 1]^+$, 348 (5) $[M + 1-CO]^+$, 320 (6) $[M + 1-2CO]^+$, 291 (46) $[M - 3CO]^+$, 263 (45) $[M - 4CO]^+$, 207 (100) $[M - Fe(CO)_4]^+$. HR-MS (FAB $^+$) m/z for $C_{16}H_{13}FeNO$ $[M - 3CO]^+$: calculated 291.0347, found 291.0341.

η^4 -[(E)-2-(4-Bromophenyl)-4-(pyridin-2-yl)-1,3-butadien-1-one]tricarbonyliron(0) (3c). Orange solid (78%). m.p. (dec.) 108–109 °C. ATR-FTIR ν (cm $^{-1}$): 2064, 2012, 1982 (C=O)_{metallic}, 1729 (C=O)_{ketene}. 1 H-NMR (300 MHz, CDCl $_3$) δ (ppm): 8.61 (d, J = 4.6 Hz, 1H), 7.66–7.45 (m, 5H), 7.41 (d, J = 8.2 Hz, 1H), 7.23 (d, J = 7.7 Hz, 1H), 7.19–7.09 (m, 1H), 3.28 (d, J = 8.2 Hz, 1H). 13 C-NMR (75 MHz, CDCl $_3$) δ (ppm): 233.0, 157.2, 150.0, 137.0, 132.6, 130.4, 129.0, 123.2, 122.1, 94.1, 58.1, 49.7. MS (FAB $^+$) m/z (%): 442, 440 (4) $[M + 1]^+$, 414, 412 (6) $[M + 1-CO]^+$, 357, 355 (35) $[M - 3CO]^+$, 329, 327 (63) $[M - 4CO]^+$, 273, 271 (20) $[M - Fe(CO)_4]^+$. HR-MS (FAB $^+$) m/z for $C_{15}H_{10}BrFeNO$ $[M - 3CO]^+$: calculated 354.9295, found 354.9291.

η^4 -[(E)-2-(4-Iodophenyl)-4-(pyridin-2-yl)-1,3-butadien-1-one]tricarbonyliron(0) (3d). Orange solid (59%). m.p. (dec.) 124–126 °C. ATR-FTIR ν (cm $^{-1}$): 2060, 2005, 1986 (C=O)_{metallic}, 1736 (C=O)_{ketene}. 1 H-NMR (300 MHz, CDCl $_3$) δ (ppm): 8.62 (d, J = 3.9 Hz, 1H), 7.73 (d, J = 8.0 Hz, 2H), 7.62 (t, J = 7.6 Hz, 1H), 7.65–7.59 (m, 3H), 7.25 (m, 1H), 7.21–7.12 (m, 1H), 3.29 (d, J = 8.4 Hz, 1H). 13 C-NMR (75 MHz, CDCl $_3$) δ (ppm): 233.0, 157.1, 150.0, 138.5, 137.0, 131.0, 129.1, 123.2, 122.1, 94.8, 94.0, 58.2, 49.9. MS (FAB $^+$) m/z (%): 488 (4) $[M + 1]^+$, 403 (15) $[M - 3CO]^+$, 375 (42) $[M - 4CO]^+$, 319 (12) $[M - Fe(CO)_4]^+$. HR-MS (FAB $^+$) m/z for $C_{15}H_{10}IFeNO$ $[M - 3CO]^+$: calculated 402.9157, found 402.9157.

η^4 -[(E)-4-(Pyridin-2-yl)-2-(trifluoromethyl)phenyl]buta-1,3-dien-1-one]tricarbonyliron(0) (3e). Orange solid (47%). m.p. (dec.) 83–87 °C. ATR-FTIR ν (cm $^{-1}$): 2069, 2003, 1985 (C=O)_{metallic}, 1745 (C=O)_{ketene}, 1321, 1113, 1067, 838. 1 H-NMR (300 MHz, CDCl $_3$) δ (ppm): 8.64 (d, J = 2.4 Hz, 1H), 7.78–7.63 (m, 5H), 7.48 (d, J = 8.3 Hz, 1H), 7.27–7.18 (m, 2H), 3.35 (d, J = 8.3 Hz, 1H). 13 C-NMR (75 MHz, CDCl $_3$) δ (ppm): 232.3, 156.9, 150.1, 137.0, 136.0, 130.7 (q, J = 32.9 Hz, CCF $_3$), 127.8, 126.3 (q, J = 3.7 Hz, CHCCF $_3$), 124.0 (q, J = 272.2 Hz, CF $_3$), 123.2, 122.3, 94.5, 58.7, 48.8. MS (FAB $^+$) m/z (%): 430 (5) $[M + 1]^+$, 402 (4) $[M + 1-CO]^+$, 374 (7) $[M + 1-2CO]^+$, 345 (87) $[M - 3CO]^+$, 317 (75) $[M - 4CO]^+$, 262 (100) $[M - Fe(CO)_4]^+$. HR-MS (FAB $^+$) m/z for $C_{16}H_{10}F_3FeNO$ $[M - 3CO]^+$: calculated 345.0064, found 345.0064.

η^4 -[(E)-2-(4-Methoxyphenyl)-4-(pyridin-2-yl)-1,3-butadien-1-one]tricarbonyliron(0) (3f). Orange solid (80%). m.p. (dec.) 116–118 °C. ATR-FTIR ν (cm $^{-1}$): 2091, 2060, 2005, 1981 (C=O)_{metallic}, 1741 (C=O)_{ketene}. 1 H-NMR (300 MHz, CDCl $_3$) δ (ppm): 8.62 (d, J = 3.7 Hz, 1H), 7.63–7.56 (m, 3H), 7.30 (d, J = 8.3 Hz, 1H), 7.23 (d, J = 7.7 Hz, 1H), 7.37 (m, 1H), 6.93 (d, J = 8.6 Hz, 2H), 3.84 (s, 3H), 3.24 (d, J = 8.3 Hz, 1H). 13 C-NMR (75 MHz, CDCl $_3$) δ (ppm): 234.8, 160.4, 157.8, 149.9, 136.9, 129.0, 123.1, 122.0, 121.9, 115.0, 93.5, 57.4, 55.5, 51.9. MS (FAB $^+$) m/z (%): 392 (6) $[M + 1]^+$, 364 (4) $[M + 1-CO]^+$, 335 (7) $[M + 1-2CO]^+$, 307 (78) $[M - 3CO]^+$, 279 (63) $[M - 4CO]^+$, 223 (84) $[M - Fe(CO)_4]^+$. HR-MS (FAB $^+$) m/z for $C_{16}H_{13}FeNO_2$ $[M - 3CO]^+$: calculated 307.0296, found 307.0298.

η^4 -[(E)-2-([1,1'-Biphenyl]-4-yl)-4-(pyridin-2-yl)-1,3-butadien-1-one]tricarbonyliron(0) (3g). Orange solid (77%). m.p. (dec.) 123–125 °C. ATR-FTIR ν (cm $^{-1}$): 2058, 2004, 1989 (C=O)_{metallic}, 1746 (C=O)_{ketene}. 1 H-NMR (300 MHz, CDCl $_3$) δ (ppm): 8.64 (s, 1H), 7.75–7.37 (m, 10H), 7.25 (m, 1H), 7.17 (s, 1H), 3.31 (d, J = 8.2 Hz, 1H). 13 C-NMR (75 MHz, CDCl $_3$) δ (ppm): 233.8, 157.4, 150.0, 141.8, 140.2, 136.9, 129.9, 129.0, 128.0, 127.9, 127.1, 123.2, 122.0, 94.0, 77.6, 77.2, 76.7, 58.0, 51.0. MS (FAB $^+$) m/z (%): 438 (6) $[M + 1]^+$, 410 (6) $[M + 1-CO]^+$, 353 (28) $[M - 3CO]^+$, 325 (30) $[M - 4CO]^+$, 269 (68) $[M - Fe(CO)_4]^+$. HR-MS (FAB $^+$) m/z for $C_{21}H_{15}FeNO$ $[M - 3CO]^+$: calculated 353.0503, found 353.0508.

η^4 -[(E)-2-(Naphthalen-2-yl)-4-(pyridin-2-yl)buta-1,3-dien-1-one]tricarbonyliron(0) (3h). Orange solid (83%). m.p. (dec.) 124–126 °C. ATR-FTIR ν (cm $^{-1}$): 2058, 2004, 1989 (C=O)_{metallic}, 1746 (C=O)_{ketene}. 1 H-NMR (300 MHz, CDCl $_3$) δ (ppm): 8.64

(d, $J = 4.3$ Hz, 1H), 8.20 (s, 1H), 7.95–7.76 (m, 3H), 7.70 (dd, $J = 8.6$, 1.7 Hz, 1H), 7.61 (td, $J = 7.7$, 1.7 Hz, 1H), 7.55 (d, $J = 8.4$ Hz, 1H), 7.50 (m, 2H), 7.31–7.19 (m, 1H), 7.15 (dd, $J = 7.0$, 5.2 Hz, 1H), 3.33 (d, $J = 8.4$ Hz, 1H). ^{13}C -NMR (75 MHz, CDCl_3) δ (ppm): 233.8, 157.5, 150.0, 136.9, 133.5, 133.3, 129.4, 128.2, 127.9, 127.4, 127.1, 127.0, 124.2, 123.2, 122.0, 94.1, 58.0, 50.9. MS (FAB $^+$) m/z (%): 412 (5) [M + 1] $^{+*}$, 384 (4) [M + 1-CO] $^+$, 327 (44) [M – 3CO] $^+$, 299 (50) [M – 4CO] $^+$, 243 (100) [M – Fe(CO) $_4$] $^+$. HR-MS (FAB $^+$) m/z for $\text{C}_{19}\text{H}_{13}\text{FeNO}$ [M – 3CO] $^+$: calculated 327.0347, found 327.0345.

η^4 -[(E)-2-(1-Methyl-1*H*-pyrrol-2-yl)-4-(pyridin-2-yl)buta-1,3-dien-1-one]tricarbonyliron(0) (3i). Orange solid (78%). m.p. (dec.) 102–107 °C. ATR-FTIR ν (cm $^{-1}$): 2057, 2004, 1979 (C=O)_{metallic}, 1770 (C=O)_{ketene}, 1474, 732. ^1H -NMR (300 MHz, CDCl_3) δ (ppm): 8.60 (s, 1H), 7.58 (s, 1H), 7.34–7.04 (m, 3H), 6.70 (s, 1H), 6.48 (s, 1H), 6.15 (s, 1H), 3.80 (s, 3H), 3.09 (d, $J = 7.3$ Hz, 1H). ^{13}C -NMR (75 MHz, CDCl_3) δ (ppm): 233.0, 157.7, 149.9, 136.8, 126.6, 123.1, 121.8, 120.8, 113.6, 109.0, 94.4, 56.5, 48.2, 36.0. MS (FAB $^+$) m/z (%): 365(5) [M + 1] $^{+*}$, 337 (3) [M + 1-CO] $^+$, 308 (8) [M – 2CO] $^+$, 280 (48) [M – 3CO] $^+$, 252 (50) [M – 4CO] $^+$, 196 (20) [M – Fe(CO) $_4$] $^+$. HR-MS (FAB $^+$) m/z for $\text{C}_{14}\text{H}_{12}\text{FeN}_2\text{O}$ [M – 3CO] $^+$: calculated 280.0299, found 280.0290.

η^4 -[(E)-2-Phenyl-4-(quinolin-2-yl)buta-1,3-dien-1-one]tricarbonyliron(0) (3l). Orange solid (73%). m.p. (dec.) 100–105 °C. IR (KBr) ν (cm $^{-1}$): 2058, 1983 (C=O)_{metallic}, 1746 (C=O)_{ketene}. ^1H -NMR (300 MHz, CDCl_3) δ (ppm): 8.07 (m, 2H), 7.78 (d, $J = 8.1$ Hz, 1H), 7.69 (m, 4H), 7.50 (m, 1H), 7.41 (m, 3H), 7.32 (d, $J = 8.5$ Hz, 1H), 3.33 (d, $J = 8.3$ Hz, 1H). ^{13}C -NMR (75 MHz, CDCl_3) δ (ppm): 233.5, 157.9, 148.4, 136.8, 131.1, 130.1, 129.4, 129.1, 128.9, 127.9, 127.8, 127.1, 126.5, 121.4, 94.6, 57.5, 51.4. MS (FAB $^+$) m/z (%): 412 (5) [M + 1] $^{+*}$, 327 (45) [M + 1-3CO] $^+$, 299 (100) [M – 4CO] $^+$, 243 (95) [M – Fe(CO) $_4$] $^+$. HR-MS (FAB $^+$) m/z for $\text{C}_{19}\text{H}_{13}\text{FeNO}$ [M – 3CO] $^+$: calculated 327.0347, found 327.0351.

General procedure for the synthesis of 3-substituted 4*H*-quinolizin-4-ones 4a–l

In a 25 mL round-bottomed flask, a solution of 3 (0.5 mmol) in 10 mL of benzene was refluxed for 4 h. In most cases, the reaction mixture turned dark brown and the formation of a dark precipitate was observed during the reaction. After the reaction was complete, the crude product was filtered off through a celite column (5 cm) and the solvent was evaporated under reduced pressure using a rotary evaporator. The reaction mixture was chromatographed on a silica gel column using hexane–dichloromethane (9 : 1, v/v) as an eluent.

3-Phenyl-4*H*-quinolizin-4-one (4a). Yellow solid (77%). m.p. 131–132 °C. ATR-FTIR ν (cm $^{-1}$): 1648 (C=O), 1620 (C=C). ^1H -NMR (300 MHz, CDCl_3) δ (ppm): 9.25 (d, $J = 7.4$ Hz, 1H), 7.89–7.83 (m, 3H), 7.48–7.41 (m, 3H), 7.34–7.25 (m, 2H), 7.01 (t, $J = 7.0$ Hz, 1H), 6.74 (d, $J = 8.0$ Hz, 1H). ^{13}C -NMR (75 MHz, CDCl_3) δ (ppm): 157.3, 142.0, 137.9, 137.0, 129.2, 128.8, 128.3, 127.8, 127.1, 125.4, 120.2, 115.4, 103.4. MS (EI, 70 eV) m/z (%): 221 (86) [M] $^{+*}$, 193 (100) [M – CO] $^+$. HR-MS (FAB $^+$) m/z for $\text{C}_{15}\text{H}_{12}\text{NO}$ [M + H] $^+$: calculated 222.0919, found 222.0927.

3-(4-Methylphenyl)-4*H*-quinolizin-4-one (4b). Yellow solid (75%). m.p. 126–127 °C. ATR-FTIR ν (cm $^{-1}$): 1648 (C=O), 1621 (C=C). ^1H -NMR (300 MHz, CDCl_3) δ (ppm): 9.22 (d, $J = 7.4$ Hz, 1H), 7.85 (d, $J = 8.0$ Hz, 1H), 7.75 (d, $J = 8.1$ Hz, 2H), 7.43 (d, $J = 8.7$ Hz, 1H), 7.29–7.23 (m, 3H), 6.98 (t, $J = 6.8$ Hz, 1H), 6.70 (d, $J = 8.0$ Hz, 1H), 2.38 (s, 3H). ^{13}C -NMR (75 MHz, CDCl_3) δ (ppm): 157.2, 141.7, 136.8, 136.6, 135.0, 129.0, 128.9, 128.6, 127.6, 125.4, 120.2, 115.3, 103.4, 21.3. MS (EI, 70 eV) m/z (%): 235 (100) [M] $^{+*}$, 207 (82) [M – CO] $^+$. HR-MS (FAB $^+$) m/z for $\text{C}_{16}\text{H}_{14}\text{NO}$ [M + H] $^+$: calculated 236.1075, found 236.1072.

3-(4-Bromophenyl)-4*H*-quinolizin-4-one (4c). Yellow solid (72%). m.p. 133–134 °C. ATR-FTIR ν (cm $^{-1}$): 1650 (C=O), 1618 (C=C), 1491, 1067, 791. ^1H -NMR (300 MHz, CDCl_3) δ (ppm): 9.24 (d, $J = 7.3$ Hz, 1H), 7.84 (d, $J = 8.0$ Hz, 1H), 7.74 (d, $J = 8.5$ Hz, 2H), 7.54 (d, $J = 8.5$ Hz, 2H), 7.48 (d, $J = 8.8$ Hz, 1H), 7.44–7.30 (m, 1H), 7.04 (t, $J = 6.5$ Hz, 1H), 6.74 (d, $J = 8.0$ Hz, 1H). ^{13}C -NMR (75 MHz, CDCl_3) δ (ppm): 157.0, 142.2, 136.8, 136.6, 131.4, 130.4, 129.6, 127.8, 125.5, 121.0, 118.6, 115.7, 103.5. MS (EI, 70 eV) m/z (%): 299, 301 (100) [M] $^{+*}$, 271, 273 (63) [M – CO] $^+$. HR-MS (FAB $^+$) m/z for $\text{C}_{15}\text{H}_{11}\text{BrNO}$ [M + H] $^+$: calculated 300.0024, found 300.0031.

3-(4-Iodophenyl)-4*H*-quinolizin-4-one (4d). Yellow solid (81%). m.p. 158–159 °C. ATR-FTIR ν (cm $^{-1}$): 1648 (C=O), 1620 (C=C), 1494, 1071, 793. ^1H -NMR (300 MHz, CDCl_3) δ (ppm): 9.24 (d, $J = 7.4$ Hz, 1H), 7.85 (d, $J = 8.0$ Hz, 1H), 7.75 (d, $J = 8.4$ Hz, 2H), 7.61 (d, $J = 8.4$ Hz, 2H), 7.49 (d, $J = 8.7$ Hz, 1H), 7.43–7.30 (m, 1H), 7.05 (t, $J = 6.6$ Hz, 1H), 6.74 (d, $J = 8.0$ Hz, 1H). ^{13}C -NMR (75 MHz, CDCl_3) δ (ppm): 157.0, 142.2, 137.5, 137.4, 136.6, 130.6, 129.6, 127.8, 125.5, 118.7, 115.7, 103.5, 92.7. MS (EI, 70 eV) m/z (%): 347 (100) [M] $^{+*}$, 319 (30) [M – CO] $^+$. HR-MS (FAB $^+$) m/z for $\text{C}_{15}\text{H}_{10}\text{INO}$ [M] $^+$: calculated 346.9807, found 346.9806.

3-(4-Trifluoromethyl)phenyl)-4*H*-quinolizin-4-one (4e). Yellow solid (77%). m.p. 164–166 °C. ATR-FTIR ν (cm $^{-1}$): 1649 (C=O), 1625 (C=C), 1488, 1325, 1106, 1072, 799. ^1H -NMR (300 MHz, CDCl_3) δ (ppm): 9.26 (d, $J = 7.1$ Hz, 1H), 7.98 (d, $J = 7.7$ Hz, 2H), 7.89 (d, $J = 8.0$ Hz, 1H), 7.67 (d, $J = 7.8$ Hz, 2H), 7.51 (d, $J = 8.6$ Hz, 1H), 7.38 (t, $J = 7.5$ Hz, 1H), 7.07 (t, $J = 6.5$ Hz, 1H), 6.76 (d, $J = 7.9$ Hz, 1H). ^{13}C -NMR (75 MHz, CDCl_3) δ (ppm): 157.0, 142.6, 141.6, 137.1, 130.1, 128.9, 128.8 (q, $J = 32.6$ Hz, CF_3), 127.9, 125.5, 125.2 (q, $J = 3.7$ Hz, CHCCF_3), 124.5 (q, $J = 270.0$ Hz, CF_3), 118.1, 115.9, 103.6. MS (EI, 70 eV) m/z (%): 289 (74) [M] $^{+*}$, 261 (100) [M – CO] $^+$. HR-MS (FAB $^+$) m/z for $\text{C}_{16}\text{H}_{10}\text{F}_3\text{NO}$ [M] $^+$: calculated 289.0714, found 289.0714.

3-(4-Methoxyphenyl)-4*H*-quinolizin-4-one (4f). Yellow solid (81%). m.p. 141–142 °C. ATR-FTIR ν (cm $^{-1}$): 1643 (C=O), 1619 (C=C), 1273, 1027, 809. ^1H -NMR (300 MHz, CDCl_3) δ (ppm): 9.22 (d, $J = 7.4$ Hz, 1H), 7.85–7.79 (m, 3H), 7.44 (d, $J = 8.8$ Hz, 1H), 7.27 (t, $J = 7.7$ Hz, 1H), 7.00–6.96 (m, 3H), 6.72 (d, $J = 8.0$ Hz, 1H), 3.84 (s, 3H). ^{13}C -NMR (75 MHz, CDCl_3) δ (ppm): 158.8, 157.2, 141.4, 136.2, 130.3, 129.9, 128.7, 127.5, 125.4, 120.0, 115.3, 113.8, 103.5, 55.4. MS (EI, 70 eV) m/z (%): 251 (100) [M] $^{+*}$, 236 (20) [M – CH $_3$] $^+$, 223 (30) [M – CO] $^+$, 208 (68) [M – CH $_3\text{CO}$] $^+$. HR-MS (FAB $^+$) m/z for $\text{C}_{16}\text{H}_{14}\text{NO}_2$ [M + H] $^+$: calculated 251.1025, found 251.1029.

3-[(1,1'-Biphenyl)-4-yl]-4H-quinolizin-4-one (4g). Yellow solid (78%). m.p. 187–188 °C. ATR-FTIR ν (cm⁻¹): 1647 (C=O), 1622 (C=C), 1071, 772, 690. ¹H-NMR (300 MHz, CDCl₃) δ (ppm): 9.27 (d, J = 7.3 Hz, 1H), 7.96–7.91 (m, 3H), 7.69–7.63 (m, 4H), 7.47–7.42 (m, 3H), 7.36–7.28 (m, 2H), 7.02 (t, J = 6.5 Hz, 1H), 6.75 (d, J = 8.0 Hz, 1H). ¹³C-NMR (75 MHz, CDCl₃) δ (ppm): 157.3, 142.0, 141.1, 139.8, 137.0, 136.7, 129.3, 129.2, 128.9, 127.8, 127.3, 127.2, 127.1, 125.5, 119.6, 115.5, 103.5. MS (EI, 70 eV) m/z (%): 297 (100) [M]⁺, 269 (80) [M – CO]⁺. HR-MS (FAB⁺) m/z for C₂₁H₁₅NO [M]⁺: calculated 297.1154, found 297.1146.

3-(Naphthalen-2-yl)-4H-quinolizin-4-one (4h). Yellow solid (79%). m.p. 220–221 °C. ATR-FTIR ν (cm⁻¹): 1653 (C=O), 1618 (C=C), 1484, 1288, 790, 745. ¹H-NMR (300 MHz, CDCl₃) δ (ppm): 9.23 (s, 1H), 8.30 (s, 1H), 7.99–7.67 (m, 5H), 7.41 (s, 3H), 7.28 (s, 1H), 6.98 (s, 1H), 6.74 (s, 1H). ¹³C-NMR (75 MHz, CDCl₃) δ (ppm): 157.4, 142.1, 137.2, 135.4, 133.7, 132.7, 129.4, 128.4, 127.8, 127.7, 127.7, 127.6, 127.0, 126.0, 125.9, 125.5, 120.0, 115.6, 103.6. MS (EI, 70 eV) m/z (%): 271 (100) [M]⁺, 243 (78) [M – CO]⁺. HR-MS (FAB⁺) m/z for C₁₉H₁₃NO [M]⁺: calculated 271.0997, found 271.0997.

3-(1-Methyl-1*H*-pyrrol-2-yl)-4H-quinolizin-4-one (4i). Yellow solid (79%). m.p. 129–130 °C. ATR-FTIR ν (cm⁻¹): 1643 (C=O), 1622 (C=C), 1529, 1491, 1300, 1073, 696. ¹H-NMR (300 MHz, CDCl₃) δ (ppm): 9.20 (d, J = 7.4 Hz, 1H), 7.74 (d, J = 7.9 Hz, 1H), 7.48 (d, J = 8.8 Hz, 1H), 7.38–7.29 (m, 1H), 7.01 (t, J = 6.9 Hz, 1H), 6.76 (s, 1H), 6.70 (d, J = 7.9 Hz, 1H), 6.27–6.14 (m, 2H), 3.65 (s, 3H). ¹³C-NMR (75 MHz, CDCl₃) δ (ppm): 157.0, 142.1, 139.0, 131.0, 129.2, 127.5, 125.5, 123.5, 115.4, 113.9, 110.0, 107.8, 103.1, 35.3. MS (EI, 70 eV) m/z (%): 224 (100) [M]⁺, 196 (13) [M – CO]⁺, 181 (18) [M – CH₃CO]⁺. HR-MS (FAB⁺) m/z for C₁₄H₁₂N₂O [M]⁺: calculated 225.1028, found 225.1034.

3-(Furan-2-yl)-4H-quinolizin-4-one (4j). Yellow solid (83%). m.p. 115–117 °C. IR (KBr) ν (cm⁻¹): 1660 (C=O), 1626 (C=C), 1476, 1313, 740. ¹H-NMR (300 MHz, CDCl₃) δ (ppm): 9.22 (d, J = 6.9 Hz, 1H), 8.23 (d, J = 8.1 Hz, 1H), 7.48 (s, 2H), 7.42 (d, J = 9.9 Hz, 1H), 7.28 (m, 1H), 7.02 (m, 1H), 6.75 (d, J = 8.1 Hz, 1H), 6.56 (s, 1H). ¹³C-NMR (75 MHz, CDCl₃) δ (ppm): 154.6, 150.6, 141.5, 140.8, 131.9, 128.8, 127.4, 125.6, 115.7, 112.3, 111.5, 109.7, 103.8. MS (EI, 70 eV) m/z (%): 211 (100) [M]⁺, 183 (20) [M – CO]⁺, 154 (88) [C₁₁H₈N]⁺. HR-MS (FAB⁺) m/z for C₁₃H₁₀NO₂ [M + H]⁺: calculated 212.0712, found 212.0705.

3-(Thiophen-2-yl)-4H-quinolizin-4-one (4k). Yellow solid (76%). m.p. 108–110 °C. ATR-FTIR ν (cm⁻¹): 1643 (C=O), 1619 (C=C), 1482, 1072, 786, 728. ¹H-NMR (300 MHz, CDCl₃) δ (ppm): 9.24 (d, J = 6.7 Hz, 1H), 8.15 (d, J = 7.9 Hz, 1H), 7.67 (s, 1H), 7.45 (d, J = 8.3 Hz, 1H), 7.36 (s, 1H), 7.30 (m, 1H), 7.12 (s, 1H), 7.04 (m, 1H), 6.74 (d, J = 7.8 Hz, 1H). ¹³C-NMR (75 MHz, CDCl₃) δ (ppm): 155.4, 140.8, 139.2, 132.8, 129.0, 127.7, 126.6, 126.0, 125.5, 123.1, 116.0, 114.4, 103.9. MS (EI, 70 eV) m/z (%): 27 (100) [M]⁺, 199 (74) [M – CO]⁺, 154 (20) [C₁₁H₈N]⁺. HR-MS (FAB⁺) m/z for C₁₃H₁₀NOS [M + H]⁺: calculated 228.0483, found 22.0486.

2-Phenyl-1*H*-pyrido[1,2-*a*]quinolin-1-one (4l). Yellow solid (83%). m.p. 194–195 °C. IR (KBr) ν (cm⁻¹): 1646 (C=O), 1618 (C=C), 1534, 833, 696. ¹H-NMR (300 MHz, CDCl₃) δ (ppm):

9.90 (d, J = 8.6 Hz, 1H), 7.77 (d, J = 7.6 Hz, 2H), 7.64 (d, J = 7.4 Hz, 1H), 7.58–7.29 (m, 6H), 7.25 (d, J = 9.1 Hz, 1H), 7.01 (d, J = 9.2 Hz, 1H), 6.53 (d, J = 7.4 Hz, 1H). ¹³C-NMR (75 MHz, CDCl₃) δ (ppm): 163.4, 141.3, 138.0, 136.2, 135.9, 129.5, 129.1, 128.3, 128.2, 127.9, 127.7, 127.5, 126.5, 126.5, 123.9, 122.6, 105.8. MS (EI, 70 eV) m/z (%): 271 (86) [M]⁺, 243 (100) [M – CO]⁺, 121 (24) [C₁₂H₈O]⁺. HR-MS (FAB⁺) m/z for C₁₉H₁₃NO [M]⁺: calculated 271.0997, found 271.0997.

Acknowledgements

The authors would like to acknowledge the technical assistance provided by Martin Cruz Villafañe, Luis Velasco and Javier Pérez. We would also like to thank the DGAPA IB200312-2 and CONACYT 129855 projects and CONACYT for the Ph.D. grant extended to A. R.-S (227146).

References

- (a) J. J. Vaquero and J. Alvarez-Builla, Heterocycles Containing a Ring-Junction Nitrogen, in *Modern Heterocyclic Chemistry*, ed. J. Alvarez-Builla, J. Vaquero and J. Barluenga, Wiley-VCH, Weinheim, 2011, vol. 4, pp. 1989–2070; (b) A. R. Katritzky, C. Rees and E. F. V. Scriven, Fused Five- and Six-membered Rings with Ring Junction Heteroatoms, in *Comprehensive Heterocyclic Chemistry II*, ed. G. Jones, Elsevier Science, Ltd, Oxford, vol. 8, 1996; (c) W. S. Hamama and H. H. Zoorob, *Tetrahedron*, 2002, **58**, 6143; (d) J. Elsner, F. Boeckler, K. Davidson, D. Sugden and P. Gmeiner, *Bioorg. Med. Chem.*, 2006, **14**, 1949; (e) R. Teja, S. Kapu, S. Kadiyala, V. Dhanapal and A. N. Raman, *J. Saudi Chem. Soc.*, 2013, DOI: 10.1016/j.jscs.2012.12.011; (f) M. Amir, H. Kumar and S. A. Javed, *Eur. J. Med. Chem.*, 2008, **43**, 2056; (g) M. Decker, F. Krauth and J. Lehmann, *Bioorg. Med. Chem.*, 2006, **14**, 1966; (h) M. Józán and K. Takács-Novák, *Int. J. Pharm.*, 1997, **159**, 233.
- (a) B. Ledoussal, E. H. Xiufeng, J.-I. Almstead and J. L. Gray, WO 2004014893, The Procter & Gamble Company, USA, 2004; *Chem. Abstr.*, 2004, **140**, 175113
- (b) R. Fukumoto, Y. Niwano, H. Kusakabe, C. Chu, H. Kimura, K. Nagasawa, S. Yanagihara, C. Hirosawa and S. Ishiduka, WO 2003029253, Sato Pharmaceutical Co., Ltd, Japan, 2003. *Chem. Abstr.*, 2003, **138**, 304266.
- Q. Li, D. T. W. Chu, A. Claiborne, C. S. Cooper, C. M. Lee, K. Raye, K. B. Berst, P. Donner, W. Wang, L. Hasvold, A. Fung, Z. Ma, M. Tufano, R. Flamm, L. L. Shen, J. Baranowski, A. Nilius, J. Alder, J. Meulbroek, K. Marsh, D. Crowell, Y. Hui, L. Seif, L. M. Melcher, R. Henry, S. Spanton, R. Faghih, L. Klein, S. K. Tanaka and J. J. Plattner, *J. Med. Chem.*, 1996, **39**, 3070.
- (a) Y. Kitaura, T. Oku, H. Hirai, T. Yamamoto and M. Hashimoto, U.S. Patent 4698349, Fujisawa Pharmaceutical Co., Ltd, Japan, 1987; *Chem. Abstr.*, 1988, **109**, 210913; (b) Y. Kurashina, H. Miyata and D.-I. Momose,

- EP 309260, Kissei Pharmaceutical Co., Ltd, Japan, 1989. *Chem. Abstr.*, 1989, **111**, 153656.
- 5 Y.-S. Xu, C.-C. Zeng, Z.-G. Jiao, L.-M. Hu and R.-G. Zhong, *Molecules*, 2009, **14**, 868.
- 6 (a) P. A. Otten, R. E. London and L. A. Levy, *Bioconjugate Chem.*, 2001, **12**, 203; (b) H. Komatsu, N. Iwasawa, D. Citterio, Y. Suzuki, T. Kubota, K. Tokuno, Y. Kitamura, K. Oka and K. Suzuki, *J. Am. Chem. Soc.*, 2004, **126**, 16353; (c) T. Fujii, Y. Shindo, K. Hotta, D. Citterio, S. Nishiyama, K. Suzuki and K. Oka, *J. Am. Chem. Soc.*, 2014, **136**, 2374.
- 7 W. Eberbach and W. Maier, *Tetrahedron Lett.*, 1989, **30**, 5591.
- 8 J. E. Douglas and D. A. Hunt, *J. Org. Chem.*, 1977, **42**, 3974.
- 9 (a) G. Sorsak, S. G. Grdadolnik and B. Stanovnik, *J. Heterocycl. Chem.*, 1998, **35**, 1275; (b) P. Cebasek, D. Bevk, S. Pirc, B. Stanovnik and J. Svete, *J. Comb. Chem.*, 2006, **8**, 95; (c) L. Forti, M. L. Gelmi, D. Pocar and M. Varallo, *Heterocycles*, 1986, **24**, 1401.
- 10 I. Hachiya, M. Atarashi and M. Shimizu, *Heterocycles*, 2006, **67**, 523.
- 11 R. den Heeten, L. J. P. van der Boon, D. L. J. Broere, E. Janssen, F. J. J. de Kanter, E. Ruijter and R. V. A. Orru, *Eur. J. Org. Chem.*, 2012, 275.
- 12 G. Song, D. Chen, C.-L. Pan, R. H. Crabtree and X. Li, *J. Org. Chem.*, 2010, **75**, 7487.
- 13 A. G. Birchler, F. Liu and L. S. Liebeskind, *J. Org. Chem.*, 1994, **59**, 7737.
- 14 For a comprehensive review on transition metal complexes of vinylketenes see: S. E. Gibson and M. A. Peplow, *Adv. Organomet. Chem.*, 1999, **44**, 275.
- 15 (a) N. W. Alcock, T. N. Danks, C. J. Richards and S. E. Thomas, *J. Chem. Soc., Chem. Commun.*, 1989, **21**; (b) N. W. Alcock, G. A. Pike, C. J. Richards and S. E. Thomas, *Tetrahedron: Asymmetry*, 1990, **1**, 531; (c) N. W. Alcock, C. J. Richards and S. E. Thomas, *Organometallics*, 1991, **10**, 231; (d) S. E. Gibson (née Thomas) and G. J. Tustin, *J. Chem. Soc., Perkin Trans. 1*, 1995, 2427; (e) L. Hill, C. J. Richards and S. E. Thomas, *J. Chem. Soc., Chem. Commun.*, 1990, 1085; (f) L. Hill, C. J. Richards and S. E. Thomas, *Pure Appl. Chem.*, 1992, **64**, 371; (g) K. G. Morris, S. P. Saberi and S. E. Thomas, *J. Chem. Soc., Chem. Commun.*, 1993, 209; (h) K. G. Morris, S. P. Saberi, M. M. Salter, S. E. Thomas, M. F. Ward, A. M. Z. Slawin and D. J. Williams, *Tetrahedron*, 1993, **49**, 5617; (i) S. P. Saberi, M. M. Salter, S. E. Thomas, A. M. Z. Slawin and D. J. Williams, *J. Chem. Soc., Perkin Trans. 1*, 1994, 167.
- 16 M. C. Ortega-Alfarro, A. Rosas-Sánchez, B. E. Zarate-Picazo, J. G. López-Cortés, F. Cortés-Guzmán and R. A. Toscano, *Organometallics*, 2011, **30**, 4830.
- 17 S. Bhagat, R. Sharma, D. M. Sawat, L. Sharma and A. K. Chakraborti, *J. Mol. Catal. A: Chem.*, 2006, **244**, 20.
- 18 Although coordination can be carried out with the three homoleptic iron carbonyl complexes, the use of $\text{Fe}(\text{CO})_5$ was avoided due to its high volatility and toxicity, besides the reason that the use of UV irradiation is sometimes required. On the other hand, it has been established that $\text{Fe}_2(\text{CO})_9$ is a more labile source of $[\text{Fe}(\text{CO})_4]$ than $\text{Fe}_3(\text{CO})_{12}$. Usually, $\text{Fe}_3(\text{CO})_{12}$ requires preactivation or severe reaction conditions. J. Knight and M. J. Mays, *J. Chem. Soc. A*, 1970, 654.
- 19 F. Ortega-Jiménez, M. C. Ortega-Alfarro, J. G. López-Cortés, R. A. Toscano, L. Velasco-Ibarra, E. Peña-Cabrera and C. Álvarez-Toledano, *Organometallics*, 2000, **19**, 4127.
- 20 (a) L. Hill, C. J. Richards and S. E. Thomas, *J. Chem. Soc., Chem. Commun.*, 1990, 1085; (b) C. Álvarez-Toledano, S. Hernández-Ortega, S. Bernès, R. Gutiérrez-Pérez and O. García-Mellado, *J. Organomet. Chem.*, 1997, **549**, 4.
- 21 (a) V. Boekelheide and P. Lodge Jr., *J. Am. Chem. Soc.*, 1951, **73**, 3681; (b) B. S. Thyagarajan and P. V. Gopalakrishnan, *Tetrahedron*, 1964, **20**, 1051.
- 22 (a) C. D. Johnson, *The Hammett Equation*, Cambridge University, London, 1973; (b) S. Nagaoka, Y. Shinde, K. Mukai and U. Nagashima, *J. Phys. Chem. A*, 1997, **101**, 3061; (c) J. Yang, A. Dass, A.-M. M. Rawashdeh, C. Sotiriou-Leventis, M. J. Panzner, D. S. Tyson, J. D. Kinder and N. Leventis, *Chem. Mater.*, 2004, **16**, 3457; (d) Y. Tsuno and M. Fujio, *Chem. Soc. Rev.*, 1996, **25**, 129.
- 23 (a) L. P. Hammett, *J. Am. Chem. Soc.*, 1937, **59**, 96; (b) C. Hansch, A. Leo and R. W. Taft, *Chem. Rev.*, 1991, 165.
- 24 (a) E. Speyer and M. Wolf, *Chem. Ber.*, 1927, **60**, 1424; (b) R. B. King, in *Organometallic Synthesis*, ed. J. J. Eisch and R. B. King, Academic Press, New York, vol. 1, 1965, p. 93.
- 25 G. Altomare, C. Cascarano, A. Giacovazzo, M. C. Burla, G. Polidori and M. Canalli, *J. Appl. Crystallogr.*, 1994, **27**, 435.
- 26 G. M. Sheldrick, *Acta Crystallogr., Sect. A: Found. Crystallogr.*, 2008, **64**, 112.
- 27 J. R. Lakowicz, in *Principles of Fluorescence Spectroscopy*, Plenum, New York, 1983.
- 28 J. N. Demas and G. A. Crosby, *J. Phys. Chem.*, 1971, **75**, 991.
- 29 S. Dhami, A. J. De Mello, G. Rumbles, S. M. Bishop, D. Phillips and A. Beeby, *Photochem. Photobiol.*, 1995, **61**, 341.
- 30 T. Bakó, P. Bakó, G. Keglevich, N. Báthori, M. Czugler, J. Tatai, T. Novák, G. Parlaghe and L. Tóked, *Tetrahedron: Asymmetry*, 2003, **14**, 1917.
- 31 L. E. Downs, D. M. Wolfe and P. R. Schreiner, *Adv. Synth. Catal.*, 2005, **347**, 235.
- 32 E. S. Lee, H. K. Ju, T. C. Moon, E. Lee, Y. Jahng, S. H. Lee, J. K. Son, S. H. Baek and H. W. Chang, *Biol. Pharm. Bull.*, 2004, **4**, 617.